RESULTS

RESULTS

The results obtained from the study area are described under separate heads. Results are mentioned in Tables & figures. Results indicate about the intricacies and limitations involved in the extraction of information for tropical vegetation from Hyperion data. Using two different Hyperion data sets seasonal variations are observed. Seasonal variability in reflectance spectra of dominant tree species using two different Hyperion data sets are presented as spectral profiles. Distinct absorption and reflectance pattern in the vegetation spectra of dry and post wet season imagery are represented by applying continuum removal spectra. Within species variation is characterized for *Tectona grandis* L. based on size and topography. Importance of derivative spectra in picking up the best bands for species discrimination is projected. The results also explain the importance of uniformity/homogeneity in patch size in affective accuracy assessment for wet season data. Developed confusion matrices from classified imageries are presented in tabular form. Higher accuracy using MNF band combination indicated the potential of MNF transformation to increase classification accuracy of tropical trees by reducing data dimensionality. Results from forest floor cover studies highlight the potential of Hyperion data in deciphering floor cover characteristics from soil in dry season.

For Hyperion data acquisition, two different dates were selected to demarcate the vegetation of study area by phenology as vegetation was in different stages of senescence in the month of April, 2006 (dry season) and vegetation was lush green in the month of October, 2006 (wet season).

3.1 Seasonal variability in two different Hyperion data sets

The images shown in figure 1 are displayed with bands 1649nm, 854nm and 447nm as RGB. These three band false color composites of the SWS were developed for both the data sets (dry season/wet season). This sequence of images used for subset of original and atmospherically corrected data sets. The differences in the colors of the two images (FCC) were indicative of seasonal variation coming from different acquisition dates. The most striking observation about the resulting reflectance image is that there appears to be a very weak vegetation signal across the subset of dry season data set (Figure 1a). This revealed that at the selected time of data acquisition the vegetation was with peak leaf shedding. In figure 1a, most of the areas are with weakest vegetation signals. The mountains south of the water body show up lighter white in this display combination and seem to have a no vegetation signal in dry season imagery. Whereas the wet season imagery showed healthy vegetation appearance across the subset of the satellite path in this display band combination with strong vegetation signal (Figure 1b). This revealed that at the selected time of data acquisition the vegetation was in lush green condition.

3.2 Reflectance spectra of selected tree species

Descriptive spectra were considered as pure spectral signature for selected tropical tree species. Descriptive spectra for 7 tree species such as *Dendrocalamus strictus, Ficus glomerata, Madhuca indica, Mangifera indica, Pongamia pinnata, Tectona grandis,* and *Wrightia tinctoria* were developed. Descriptive spectra for all the selected species were plotted together. Reflectance spectra of 7 tree species are shown in figure 2 with typical vegetation pattern in dry and wet season. For comparison, spectra of same pixels were extracted from the image of wet season. The differences seen amongst spectra of selected species are similar for both dry and wet seasons. Reflectance from descriptive spectra for the seven tree species such as *Tectona, Madhuca,*

Wrightia, Dendrocalamus, Mangifera, Pongamia & *Ficus* showed typical patterns of vegetation in wet season with pronounced chlorophyll absorption at 680nm, maximum reflectance at near infra-red (NIR) and low ligno- cellulose absorption in short wave infra-red (SWIR) region due to water absorptive features. Thus, green leaf spectra were dominated by the spectral features of chlorophyll and water in wet season. While in dry season species with different phenological condition had showed decreased chlorophyll absorption in visible (VIS) region and increased ligno-cellulose absorption in SWIR I & II regions of the spectrum (Figure 2). Atmospheric water absorption features prevented measurements in the 1400nm and 1900nm spectral regions for both the data sets (Figure 2).

During dry (leaf fall) season, individuals of selected tree species had very low density of crown foliage. Phenology was distinct in selected tree species. Therefore, phenological variations in the selected trees were clearly seen in the descriptive spectra (Figure 2a). *Tectona grandis* was with maximum leaf fall showing maximum reflectance in the SWIR I and SWIR II region. *Madhuca indica* was with new young leaves. *Wrightia tinctoria* was in flowering condition with sparse young foliage. These three species showed flatter reflectance spectra in the visible region of the spectrum because of the lesser to minimal chlorophyll content. *Ficus glomerata* also showed flatter reflectance pattern in VIS region as it was present with senescent old leaves. *Dendrocalamus strictus* also reflected leaf off condition and it was observed in the spectrum where slope influenced reflectance. It showed lower reflectance amongst other species. From figure 2a it was also evident that spectral reflectance varied more widely among deciduous species where greatest variation in SWIR and lowest in VIS region. Whereas among evergreen species reflectance variation was relatively small particularly in the VIS spectral region and more was in the NIR.

Deciduous species such as *Tectona, Dendrocalamus* and *Madhuca* in dry season showed lower reflectance in NIR region and lower absorption (higher reflectance) in VIS & SWIR regions of the spectrum (Figure 3). On the contrary, higher absorptions in VIS & SWIR regions and higher reflectance in NIR region was observed using wet season data. Here lower absorption in the visible region of the spectrum during dry season was a manifestation of lower chlorophyll content as compared to the wet season. With fewer or senescenced leaves in the crown, there was less photon scattering and subsequently NIR reflectance was low relative to wet season. Further

biochemical features of lignin, cellulose become more prominent in the SWIR regions of the spectrum whereas in wet season spectra these features were suppressed due to water absorption. As a result significant seasonal variability was observed in the spectral signatures of deciduous species using two different Hyperion data sets. In dry season, deciduous species had consistently higher reflectance values than evergreen species throughout the VIS region whereas lower values throughout the NIR. In figure 3 the reflectance of deciduous tree species differ greatly from evergreen species in the month of April. Species like *Mangifera indica* and *Pongamia pinnata* having a large proportion of green foliage showed different pattern of spectra. Both these species can be easily discernable in the visible region of the spectrum from other deciduous species in dry season. The evergreen species were with dense canopy closure and might be very little influence of spectral reflectance of dry vegetation in the month of April. There were no significant reflectance differences in the NIR region of *Pongamia* and *Ficus*, and in the SWIR region of *Mangifera* using two different data sets. Evergreen species showed significant difference in the reflectance at NIR (Figure 3). In wavelength longer than 1100nm, the deciduous species showed much higher reflectance compared to evergreen species.

During wet season, individuals of selected 7 tropical tree species had very high density of crown foliage. Therefore all showed typical pattern of healthy vegetation. The vegetation reflectance spectra for all the selected tropical tree species had low level of reflectance in the visible region and maximum reflectance in the NIR. This demonstrated that the spectra exhibit minimal variability in terms of magnitude in the VIS wavelengths and large rise in variability as the wavelength increased towards NIR. Highest NIR reflectance was observed in the spectra of *Mangifera indica* whereas lowest in the spectra of *Dendrocalamus strictus*. Further it was apparent that in the region of SWIR I & SWIR II water absorption features dominated biochemical characteristics.

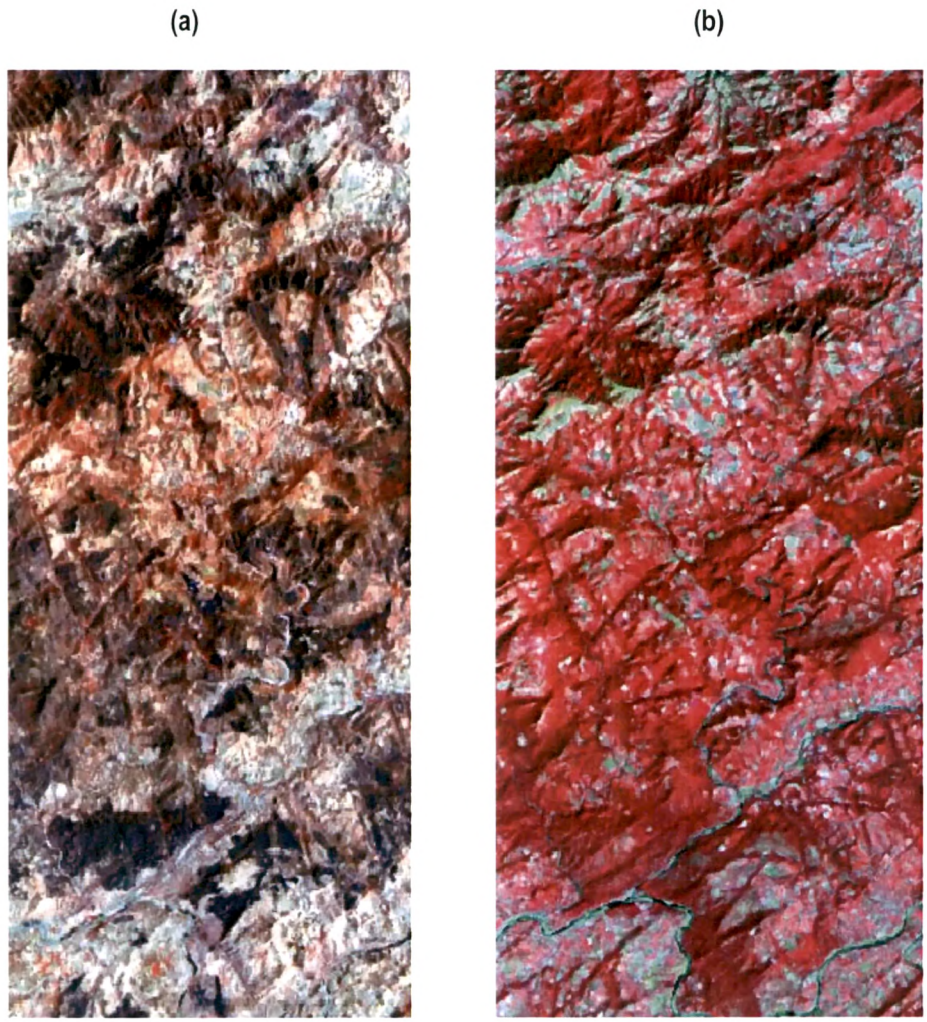

Figure 1: Atmospherically corrected subsets of Hyperion data for dry and wet season (RGB band combination - 854nm, 650nm, 559nm)

(a)

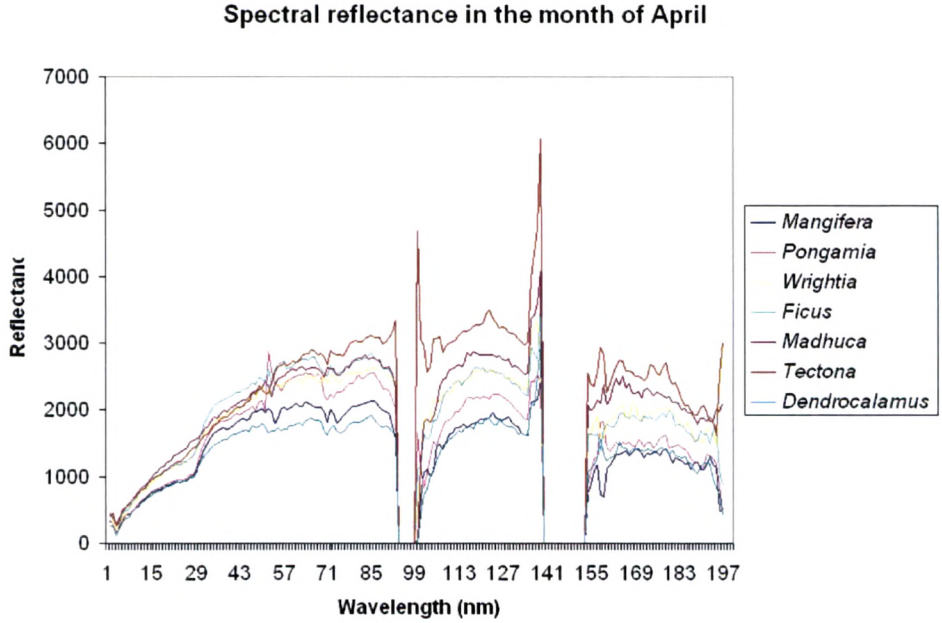

(b)

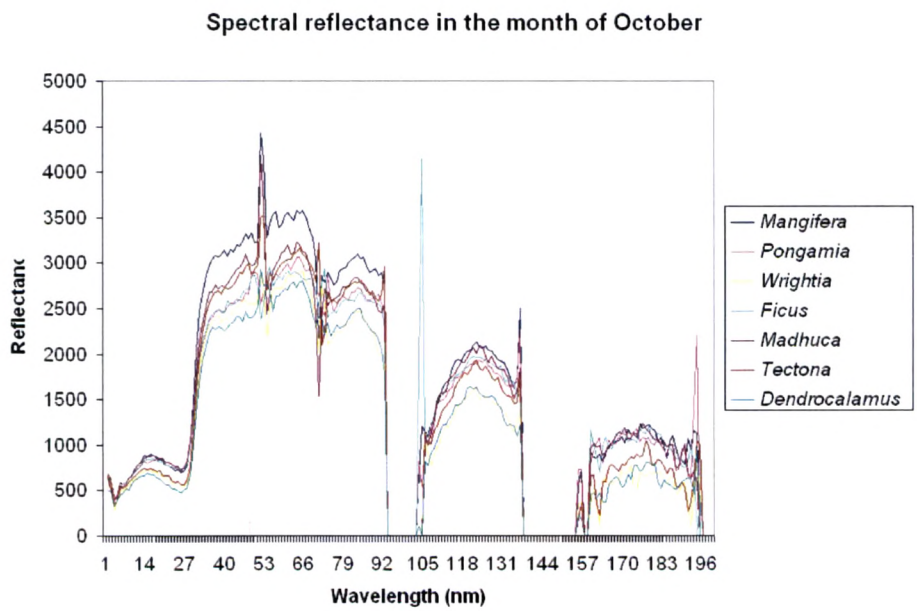

Figure 2: Reflectance spectra for the 7 species selected (a) 3rd April, 2006 and (b) 21st October, 2006

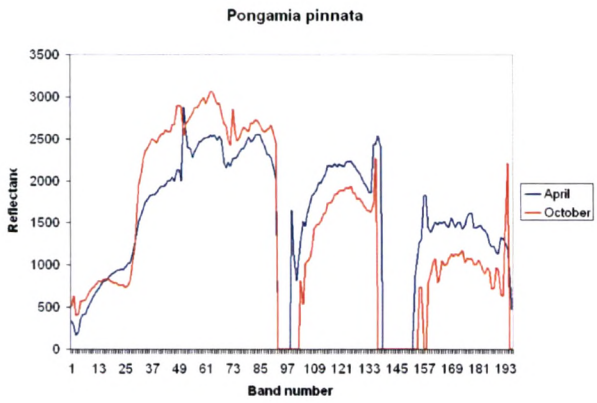
Pongamia pinnata
Reflectanc
Band number
April
October

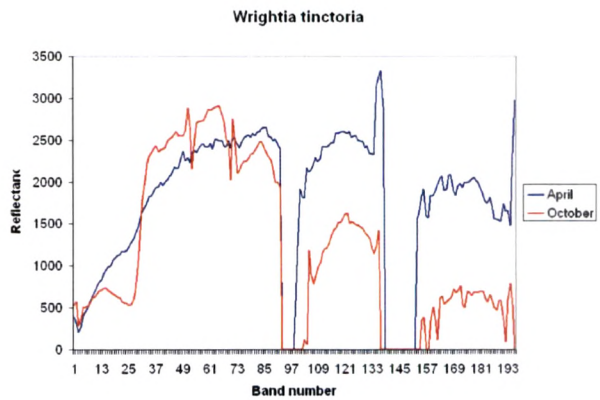
Wrightia tinctoria
Reflectanc
Band number
April
October

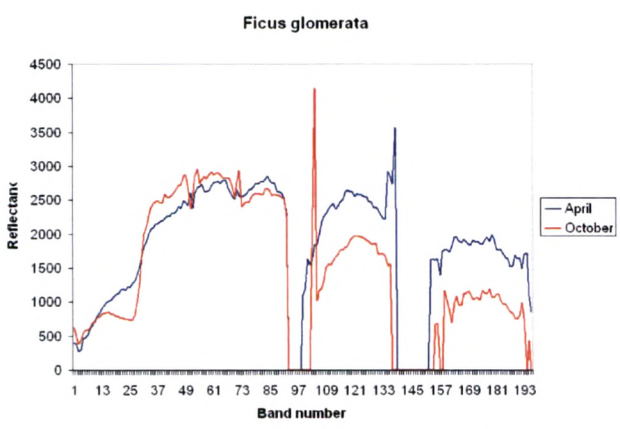
Ficus glomerata
Reflectanc
Band number
April
October

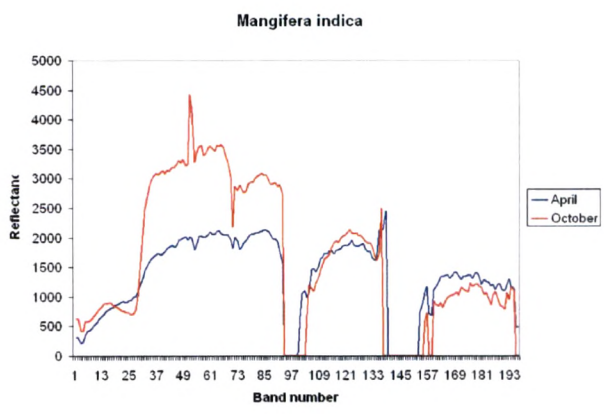
Mangifera indica
Reflectanc
Band number
April
October

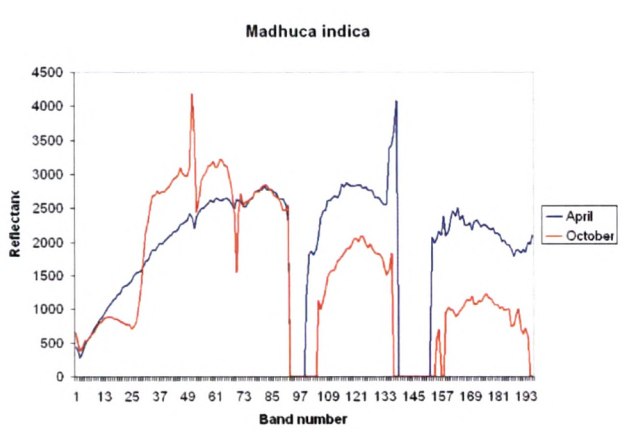
Madhuca indica
Reflectanc
Band number
April
October

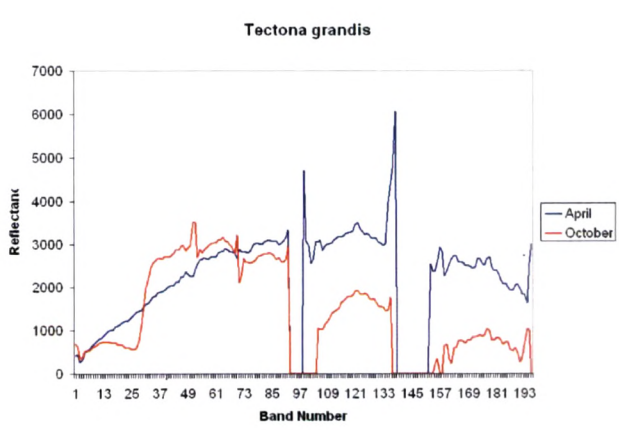
Tectona grandis
Reflectanc
Band Number
April
October

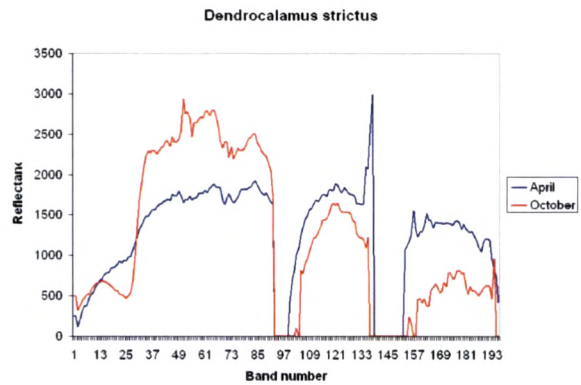

Figure 3: Reflectance spectra of the 7 tree species from two different data sets

3.3 Application of continuum removal spectra to describe distinct absorption pattern in the vegetation spectra of dry and wet season imagery

In this study the continuum removed spectra (Figure 4 a, b) showed several distinguishable absorption features in two different data sets. Spectra of 7 species showed distinct absorption features in VIS region and reflectance features in SWIR- I & SWIR-II regions of the spectrum (Figure 4 a, b). Separation was very clear at VIS and SWIR-II wavelengths. In figure 4a spectra of trees like *Pongamia*, *Mangifera* and *Ficus* from dry season showed chlorophyll absorption feature in the VIS region of the spectrum due to their phenological condition. *Pongamia* clearly showed maximum chlorophyll absorption depth. Whereas deciduous species like *Tectona* and *Dendrocalamus* demarcated lesser chlorophyll absorption features. In SWIR-II region of the spectrum, *Dendrocalamus* and *Tectona* showed maximum absorption whereas *Pongamia* showed maximum reflection. Compared to *Dendrocalamus*, *Tectona* showed lower absorption features in SWIR II region when it is completely in dry condition.

Similarly, Continuum removal also applied to the data of wet season which revealed that the *Madhuca* and *Ficus* had weaker absorption strengths compared to the *Mangifera*, *Pongamia*, *Tectona*, *Wrightia* and *Dendrocalamus*. Surprisingly, *Tectona* and *Dendrocalamus* had strongest chlorophyll absorption features (Figure 4c). From the apparent depth of an absorption feature it

was evident that *Madhuca* and *Ficus* showed lowest depth which were 0.46 and 0.44 respectively. While *Dendrocalamus*, *Tectona* and *Mangifera* showed maximum apparent chlorophyll absorption feature such as 0.70, 0.68 and 0.67 respectively. There was considerable variation in the depth of absorption feature which was likely caused by relative differences in the chlorophyll concentration between selected species. In dry season, the depth of an absorption feature was highest for *Pongamia* (0.27) while lowest or absent in *Tectona, Madhuca, Wrightia* and *Dendrocalamus*. In general, the continuum removed chlorophyll absorption features of the lush vegetation in October which was stronger in comparison to the dry vegetation in April (Figure 4). Similar to VIS region *Madhuca* and *Ficus* showed higher reflectance in SWIR-II region where *Pongamia* showed highest absorption (Figure 4b). Further figure 4b also showed narrow absorption feature at 980nm.

(a)

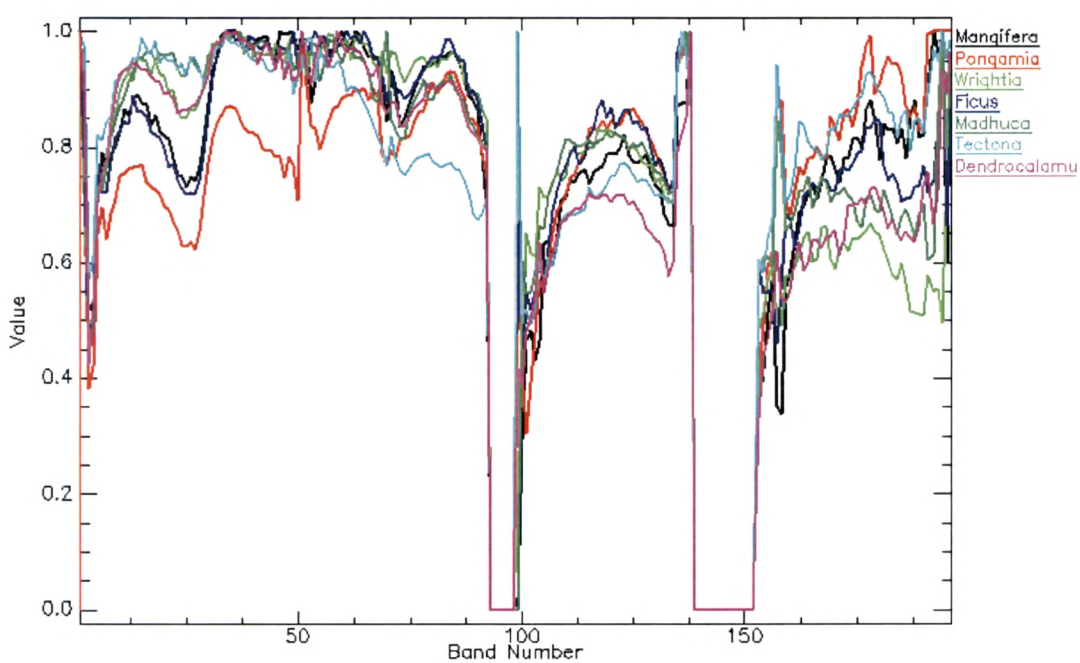

(b)

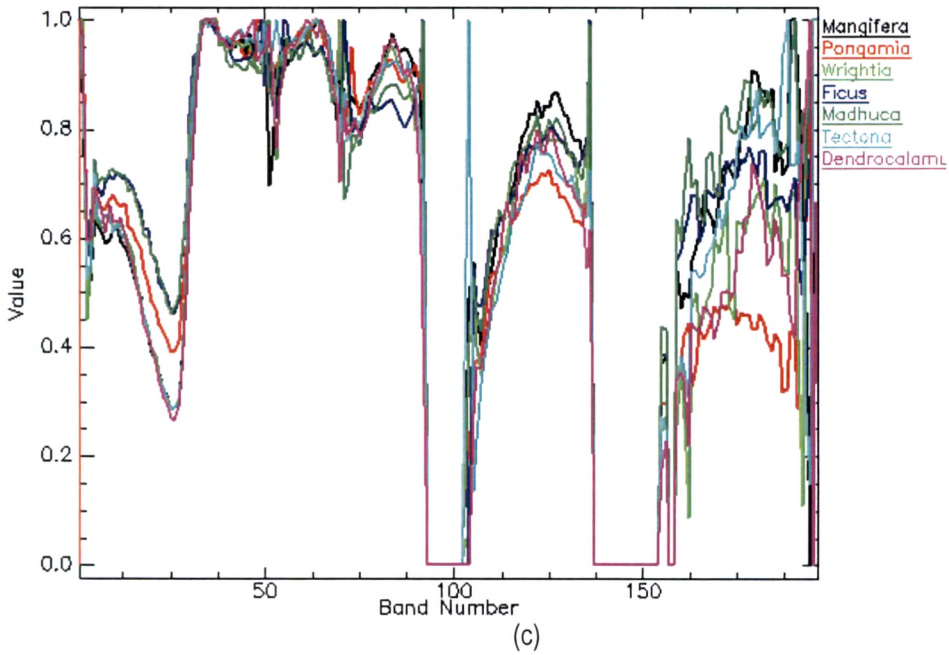

(c)

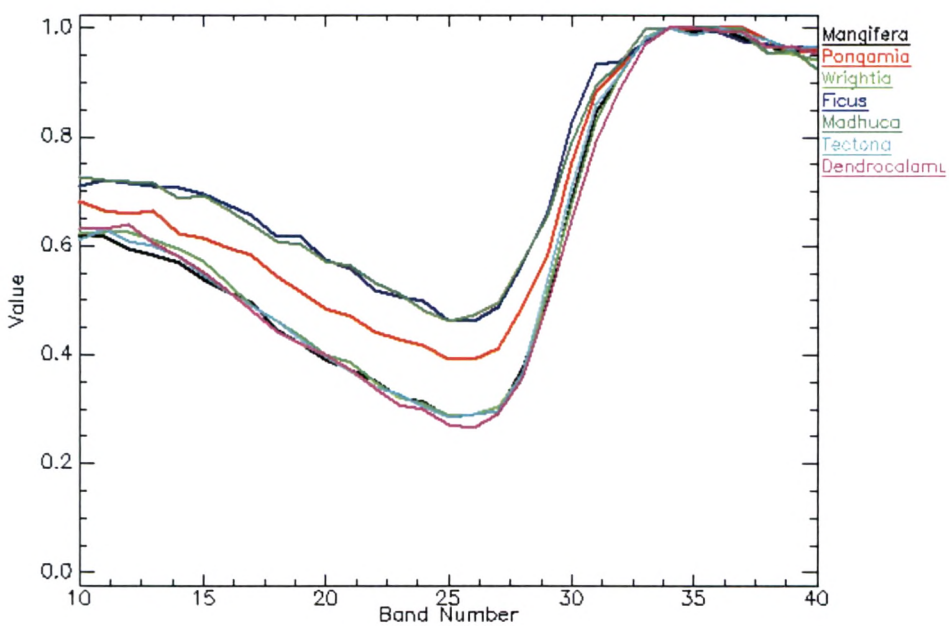

Figure 4: Continuum removal spectra for 7 different tree species from two data sets a) 9th April, 06, b) 21st October, 06 and c) Continuum removal spectra of VIS region showing chlorophyll absorption features

3.5 Intraspecies spectral variability

This section examines within species variability based on size and topography. Within species variation was distinctly observed for *Tectona* as it is dominant in the study area occupying larger area. The spectral signatures for *Tectona* from different pixels across a large area showed the same pattern of curves for dry and green condition (Figure 5). *Tectona* almost showed a denuded canopy in the month of April which was seen as lesser absorbance in the red band with a slight decrease in blue absorption (since carotenes persist and continue to absorb in the blue). Conversely, it showed a healthy canopy in the month of October which was seen as a typical vegetation signal where strong absorption in the VIS & SWIR regions due to chlorophyll and leaf water content.

The reflectance spectra of different pixels of *Tectona* showed variation based on density, the strength of canopy closure, size of trunk, and slope of area (Figure 5). From figure 5 it was evident that spectra differed as the girth varied. Variation was observed in the spectral reflectance of *Tectona* of different girth classes growing on similar area (slope) using dry season data set (Figure 5a). Whereas using wet season data, different girth classes showed similar pattern throughout the electromagnetic spectrum (Figure 5a2). Here distinct variation using dry season data among girth classes revealed significant discrimination relative to wet season. This indicates that hyperspectral data are useful in demarcating trees of the same species (similar to *Tectona*) according to their size using dry season data. From figure 5b it was observed that spectral plots of two different altitudes showed analogous reflectance in the visible region while discrepancy in NIR-SWIR region of the spectrum (dry month imagery) (Figure 5b1). Whereas in wet season it showed similar pattern throughout the electromagnetic spectrum (Figure 5b2). In figure 5c spectra were extracted from open areas with different girth class using two different data sets. Variation was observed in both spectral plots. Spectrum developed for 18-33cm girth class from dry month imagery had shown lower reflectance compared to 150-200cm girth class across all 3 regions. While 18-33 cm girth classes had shown higher reflectance in the NIR region of the spectrum as compared to 150-200cm girth class (Figure 8b) in wet month imagery. Additionally, in dry month imagery the difference in the reflectance values of *Tectona* from different pixels is maximum in SWIR-1 region of the spectrum (Figures 5a, 5b & 5c).

In order to differentiate them better the same had been plotted as continuum removal spectra. Trees with different girth classes in dry season showed different pattern (Figure 6a) and variation was observed in the SWIR-I & SWIR-II regions. While in wet season all 3 girth classes showed similar pattern in figure 6b. In figure 7a, continuum removed spectra extracted from two different altitudes showed similar pattern in dry month imagery. Altitudinal affect also was easily observed in the spectra of wet season (Figure 7b). In figure 6b maximum chlorophyll absorption in the VIS region was present in the spectrum of 50-90cm girth class where as minimum in the spectrum of 35-60cm girth class.

3.5.1. Statistical analysis

Analysis of Variance (ANOVA) performed showed that the differences seen amongst reflectance spectra of different girth classes are significant (α=.01) for both the data sets. There was a negative correlation between girth of the *Tectona* tree and corresponding reflectance spectra (r^2 = 0.7) from dry month imagery. On the contrary, there was a positive correlation between girth of the *Tectona* tree and corresponding spectra in post wet season.

(a1)

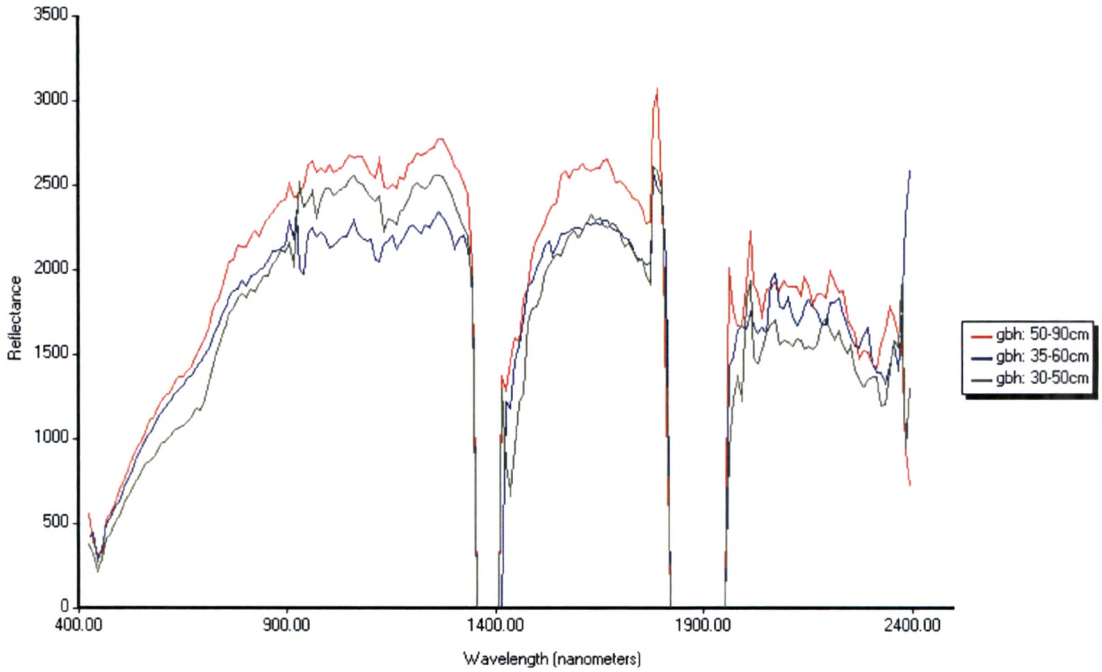
3500
3000
2500
2000
1500
1000
500
0
Reflectance
400.00
900.00
1400.00
1900.00
2400.00
Wavelength (nanometers)
gbh: 50-90cm
gbh: 35-60cm
gbh: 30-50cm

(a2)

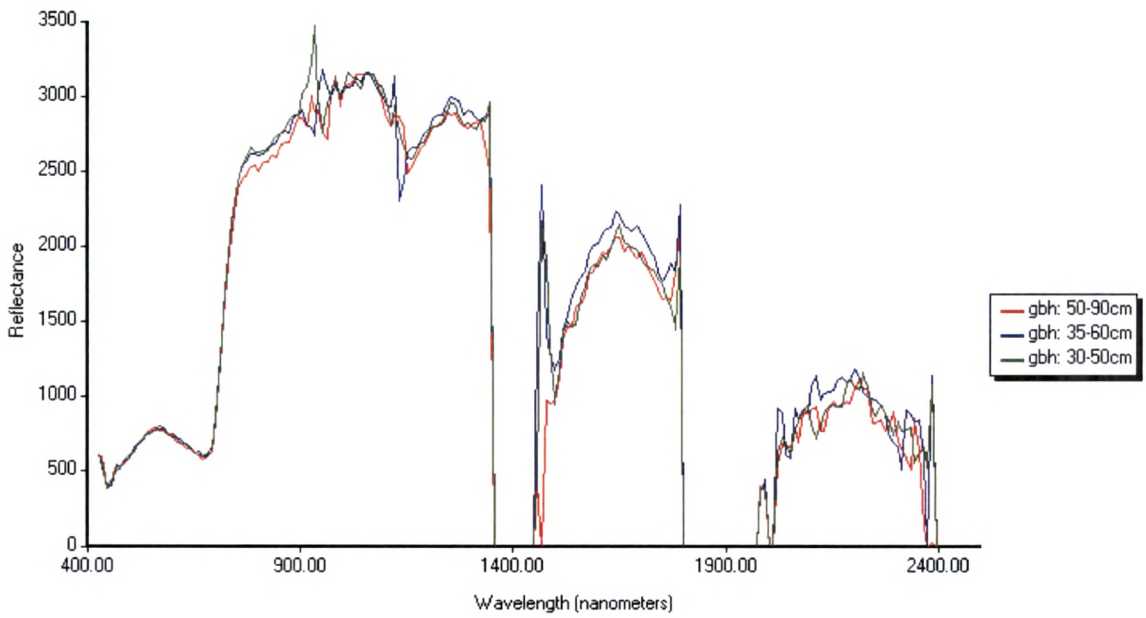
3500
3000
2500
2000
1500
1000
500
0
Reflectance
400.00
900.00
1400.00
1900.00
2400.00
Wavelength (nanometers)
gbh: 50-90cm
gbh: 35-60cm
gbh: 30-50cm

(b1)

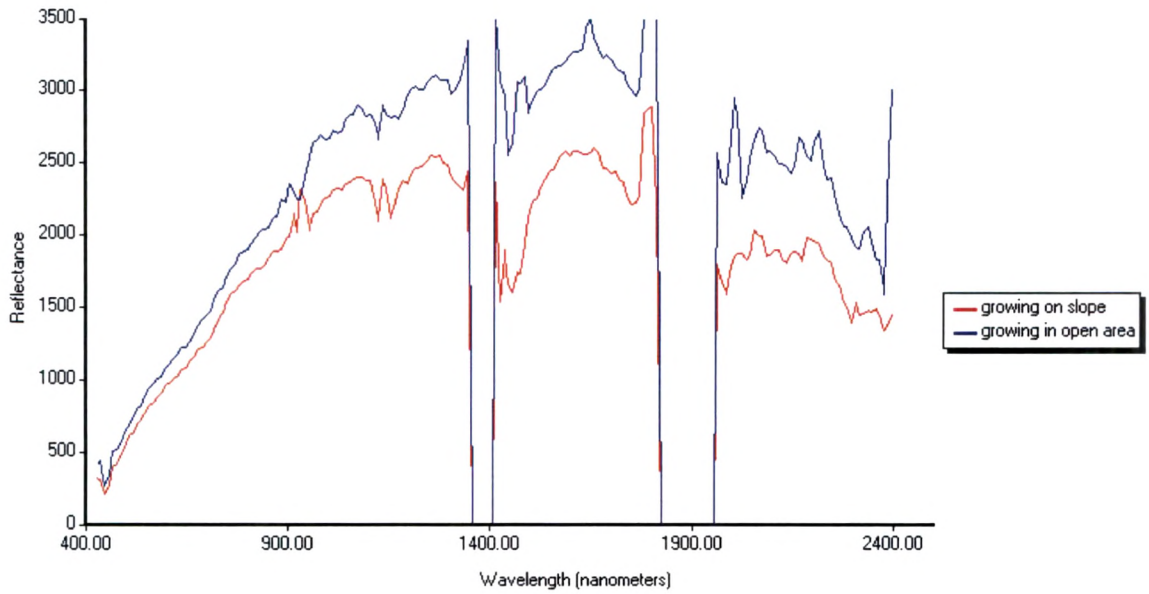
3500
3000
2500
2000
1500
1000
500
0
Reflectance
400.00
900.00
1400.00
1900.00
2400.00
Wavelength (nanometers)
growing on slope
growing in open area

(b2)

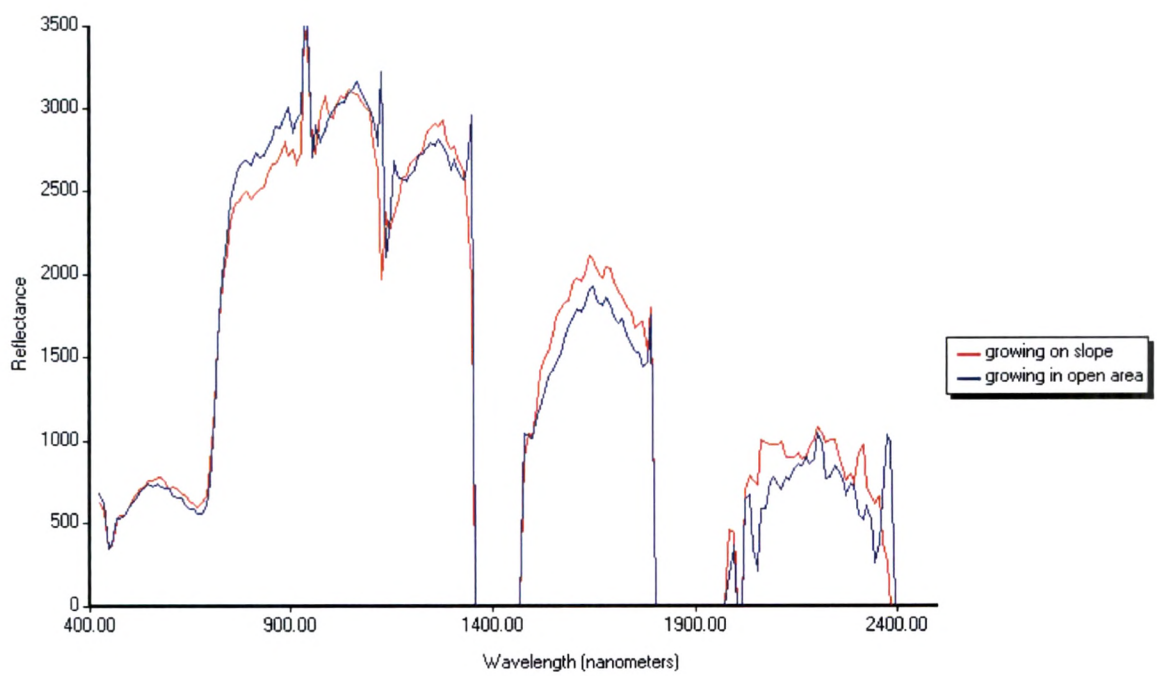
3500
3000
2500
2000
1500
1000
500
0
Reflectance
400.00
900.00
1400.00
1900.00
2400.00
Wavelength (nanometers)
growing on slope
growing in open area

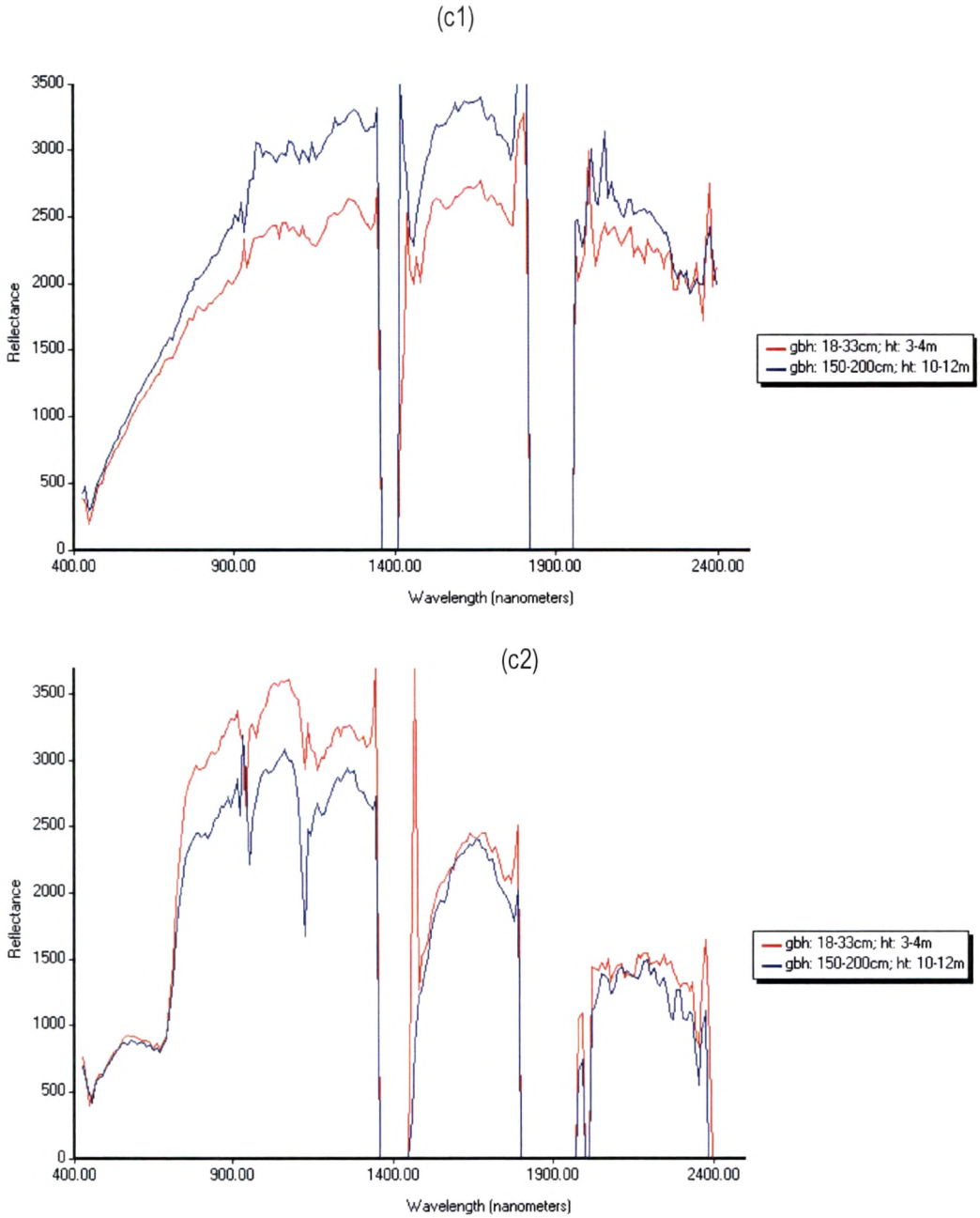

Figure 5: Spectral signature of *Tectona* a) in same terrain (Slope) with different girth classes, b) in different terrain from same girth class, c) in open areas from different girth classes. a1, b1,c1 for 9th April, 06 and a2, b2, c2 for 21st October, 06.

(a)

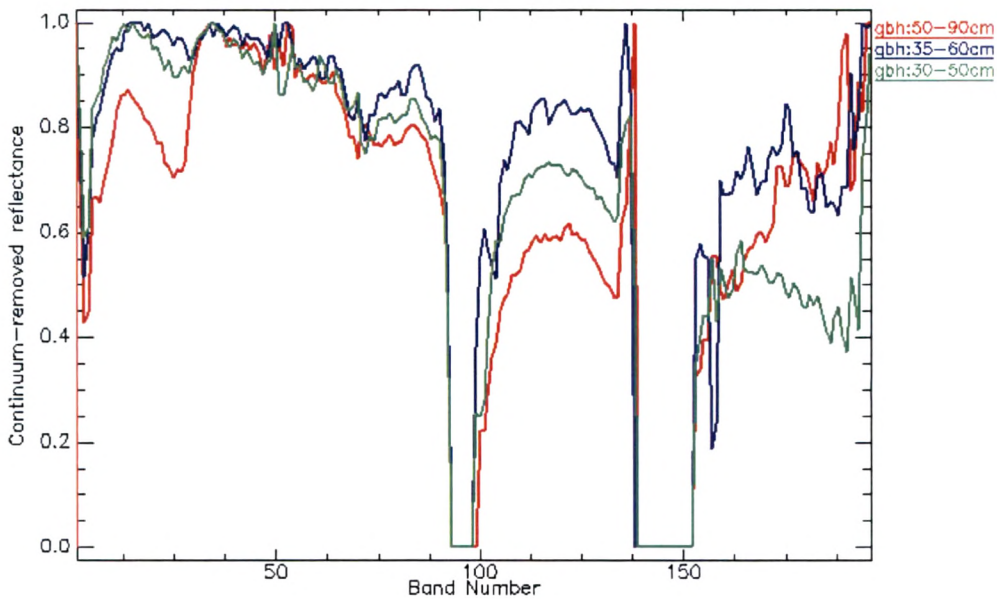

(b)

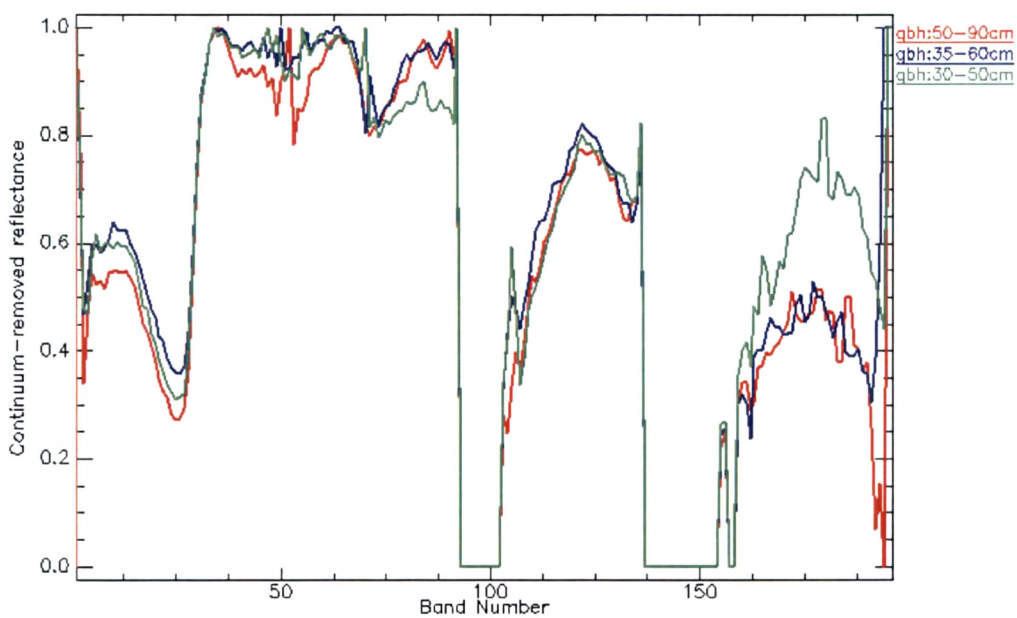

Figure 6: Continuum spectra for *Tectona* in same terrain with different girth class from two different data sets a) 3rd April, 06, b) 21st October, 06

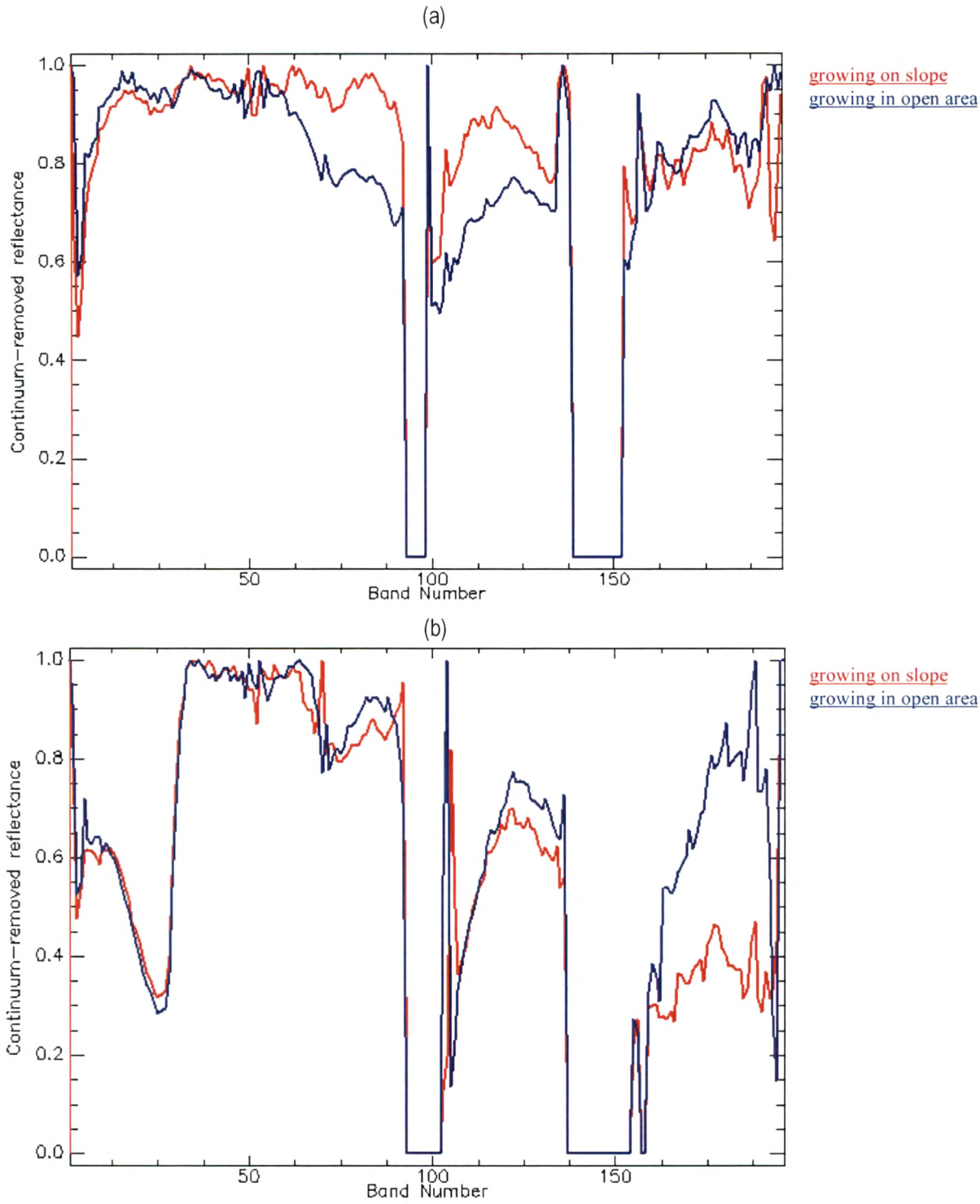

Figure 7: Continuum removal spectra of *Tectona* in different terrain with same girth class from two different data sets a) 9th April, 06, b) 21st October, 06

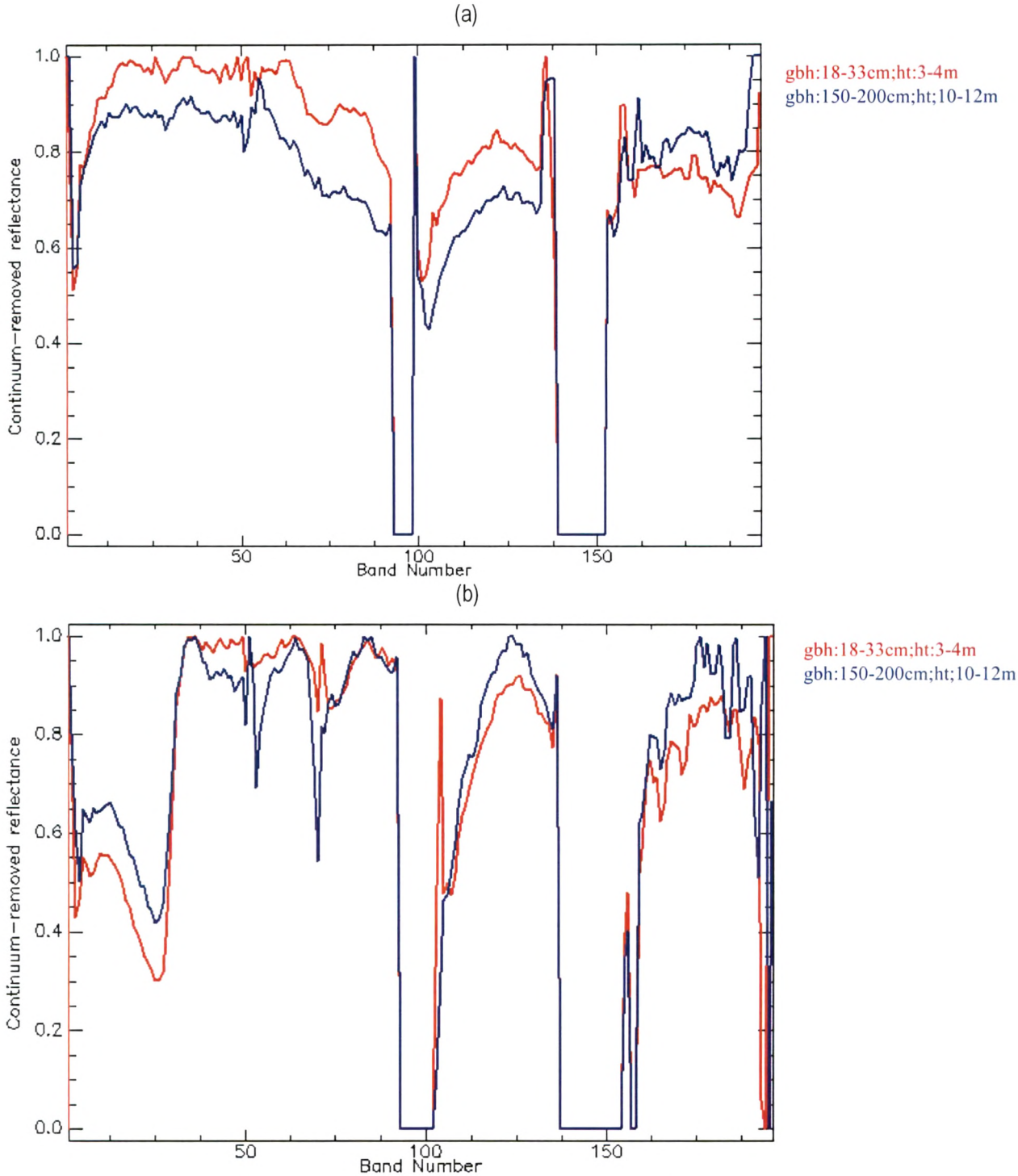

Figure 8: Continuum removal spectra for *Tectona* in open areas with different girth class from two different data sets a) 9th April, 06, b) 21st October, 06

3.6 Species level discrimination using Maximum Likelihood Classifier

This section was conducted to investigate whether high spectral reflectance data from the tropical deciduous forests of the study area during dry/summer season could be used for species level discrimination. This time was selected to discriminate evergreen and deciduous tropical vegetation based on phenological condition. Figure 2 showed the descriptive spectra for all 7 species in a single spectral profile. In this study descriptive spectra obtained were distinct for each species and phenological variations in the selected trees were clearly seen. Further in order to differentiate girth classes of *Tectona*, it was grouped into two girth classes such as Teak young (18-60cm) and Teak old (90-260cm). From figure 10 it was evident that spectra of different girth classes showed noticeable separation at all wavelengths.

3.6.1 Statistical analysis

The statistical test demonstrated whether the tropical tree species were significantly different or not. In this study spectral signature variation for each species was seen as ±1 standard deviation from the descriptive spectrum of dry month imagery (Figure 13). The one-way analysis of variance (ANOVA) performed showed that the differences seen amongst descriptive spectra were significant (α=.01). This permit the identification of tree species with different phenological stages in which greater reflectance variability was observed. Distance measurements for (D & θ) for all these spectra were estimated (Price, 1994) using *Tectona* as a reference spectra. The D & θ for each species were calculated from reflectance within 426-2395nm and presented in table 1. Since *Tectona* used as the standard, it had a nominal D & θ of zero. D values ranged from 0 to 0.75 and θ values ranged from 0 to 0.054 in radians. The values were different indicating significant differences amongst descriptive spectra of selected tree species. It was observed that decreasing D values represent an increase in reflectance magnitude while decrease in θ represents flattering of the spectral shape (Figure 2). This was evident with the spectra of *Madhuca* with lowest D & θ values where D is 0.29 and θ is 0.020 (Table 1). In this study, the results from spectral similarity measures (D & θ)) and ANOVA revealed the relative separability between selected tree species. This clearly indicated that Hyperion data is useful for separating tropical species with different phenological conditions.

Table 1: Calculated D & θ values for selected tropical tree species

Species	D value	θ value
Tectona grandis	0	0
Dendrocalamus strictus	0.24	0.031
Mangifera indica	0.75	0.054
Pongamia pinnata	0.57	0.033
Ficus glomerata	0.40	0.027
Wrightia tinctoria	0.34	0.023
Madhuca indica	0.29	0.020

3.6.2. Derivative analysis

In addition to the calibrated reflectance spectra, the derivative of the descriptive spectral signatures also were analyzed, which normalizes for brightness effects and give further information about the shape of the spectral curve. In figure 10 the ability of first derivative to enlarge differences between selected tree species were identified. The first derivative was estimated using "finite difference approximation". It was apparent that the first derivative reflection spectra were dominated by phenological variations. It displayed variation with wavelength in the slope of the original reflectance spectra. It was evident that the maxima (maximums) of first derivative spectra occurred at 701nm (The red-edge), 1396nm and 1739nm while a number of absorption peaks, revealed as local minima (minimums) were apparent at 1326nm and 1790nm. Here maxima were found by looking at the positive peaks in the first derivative spectrum, whilst the minima were detectable as negative peaks in the curves. From the derivative spectra, three bands of local maxima were selected for supervised classification.

3.6.3. The first derivative value at the red edge (dRE)

As shown in figure 11a, original reflectance spectra had almost identical pattern in red edge position (REP) (670-780nm). They differed in magnitude in the 1st derivative spectra over the same wavelength range. Several interesting spectral features were apparent in the derivative spectra that were obscure in the original spectra. For example, the double-peak features that were observed on the first derivative reflectance near 701nm and 732nm in the red-edge region (Figure 11b).

Sensitivities coming from phenological changes were understood by looking at the red-edge position (REP). The REP values for selected tree species were calculated based on linear method. From linear-four point interpolation method. Each species had different REP value. As shown in figure 11b, *Dendrocalamus* in senescent condition was associated with lower REP values whereas *Pongamia* with lush green leaves was associated with high REP value. This indicated that a difference in the REP can be a suitable parameter for species discrimination at different phenological condition. REP values were ranging from 723.03 to 725.29 for evergreen species. It was apparent that REP's of the evergreen species shift towards longer wavelength with higher reflectance than of deciduous species.

3.6.5. Species level classification

For the supervised classification, Maximum likelihood algorithm was chosen. Supervised classification of the subset using maximum likelihood classification from the three selected bands was performed. The three bands selected for classification came from red edge region (701nm) and from SWIR regions (1386nm, 1739nm) of the derivative spectra. In order to have accurate estimates of the covariance matrices per class, it was necessary to restrict the classification to 9 classes. Classified image is given in figure 12. Dominant species such as *Tectona* and *Dendrocalamus* were found to dominate the area. A sampled error matrix was calculated by comparing the field samples with the classified image. Table 3 showed the results of accuracy assessment. The boldface diagonal values indicate the number of samples in each class which were classified correctly with selected Hyperion bands. The overall accuracy of the classification was 60.7%, with 34 out of 56 samples correctly classified, with a kappa statistic of 0.57. User's accuracies, representing errors of commission and producer's accuracies, representing errors of omission were calculated for each selected classes. User's and producer's accuracies were ranging from 40 % to 80.0% and 36.3% to 100% respectively (Table- 3) indicating the potential of Hyperion imagery for the discrimination of tropical trees. Accuracy levels were lowest for *Madhuca* and showed misclassification with class "others". Accuracy levels were high for *Tectona* and *Dendrocalamus* mainly because of their larger distribution and homogeneity. Producer's accuracy was highest for Teak young (100%) followed by *Dendrocalamus* (80%). Descriptive spectra of *Tectona* showed clear variation with different sizes of girth. Supervised classification also showed clear discrimination in size classes of *Tectona*. Classification of Teak old was less reliable than

classification of Teak young with lower producer's accuracy 36.3%. From table 3 it was also apparent that deciduous and evergreen species showed lower misclassification. The above results demonstrate the potential application of techniques likes derivative spectra, and red edge position remote sensing analysis for species level discrimination using hyperspectral data.

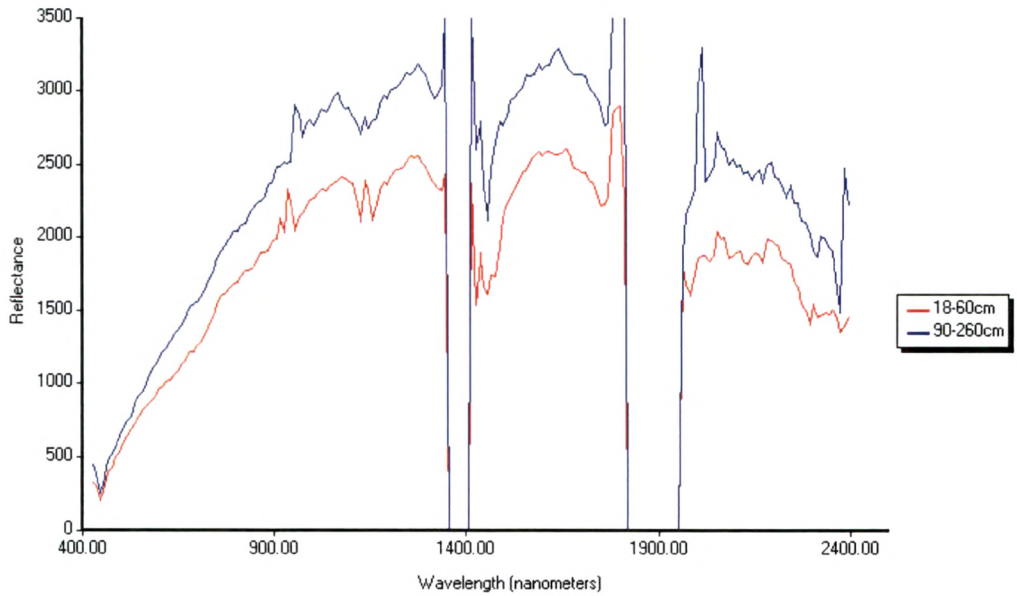

Figure 9: Descriptive spectra for different girth classes of *Tectona grandis* L.

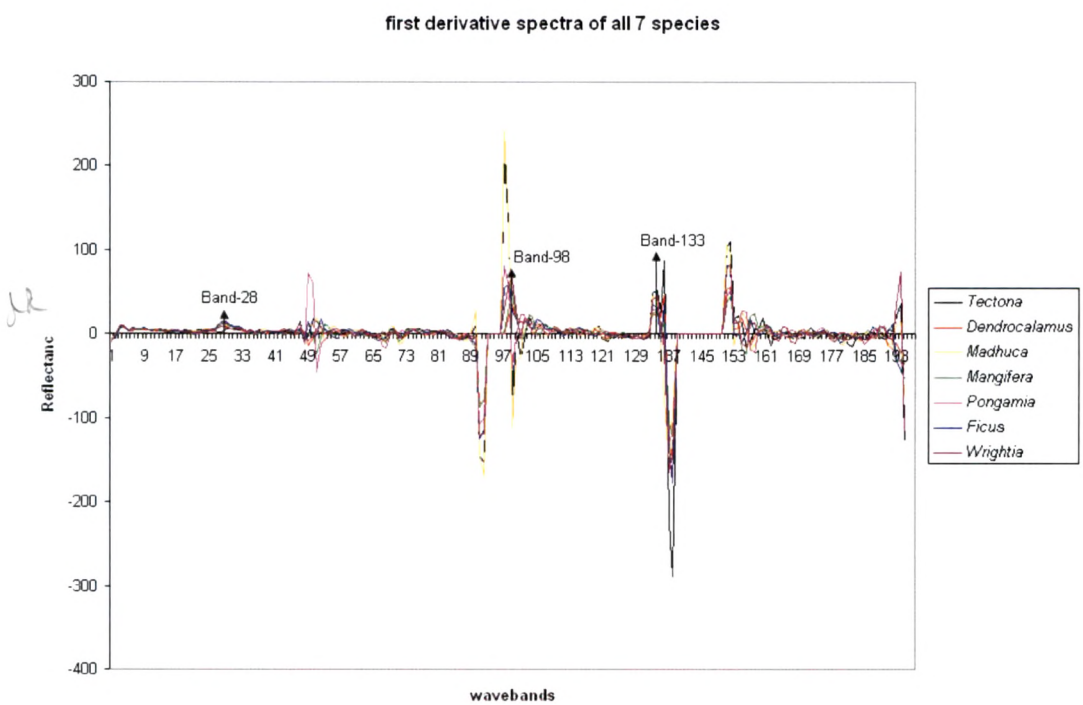

Figure 10: Derivative spectra for 7 tropical tree species using April month imagery. Arrows indicate selected bands for species level discrimination

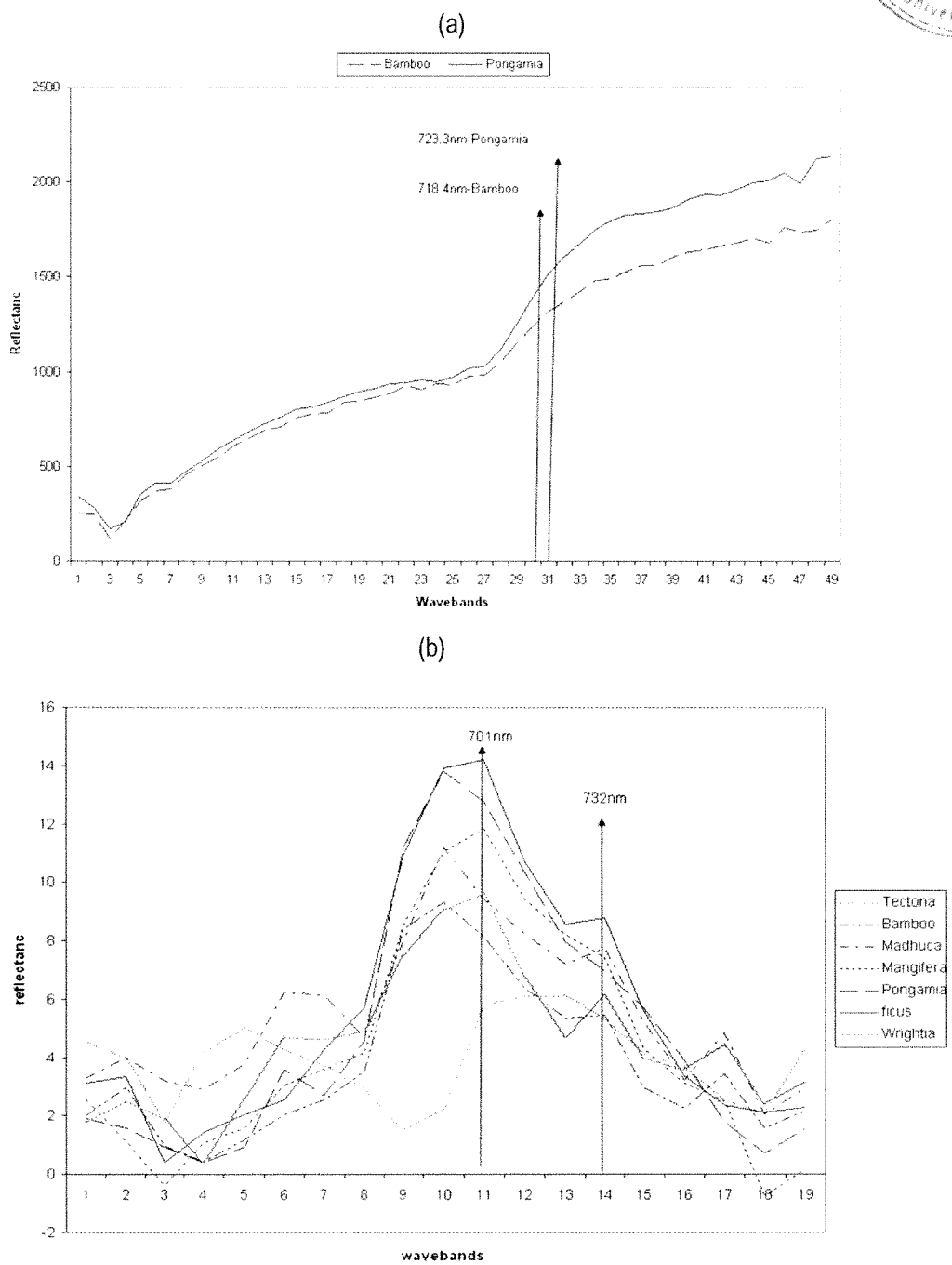

Figure 11: a) Spectral reflectance curves for *Pongamia* and *Dendrocalamus.* The red-edge inflection point shift towards lower wavelengths for *Tectona.* b) Double peak feature is apparent in the spectrally enhanced red edge region of the 1st derivative spectra as compared to the reflectance spectra.

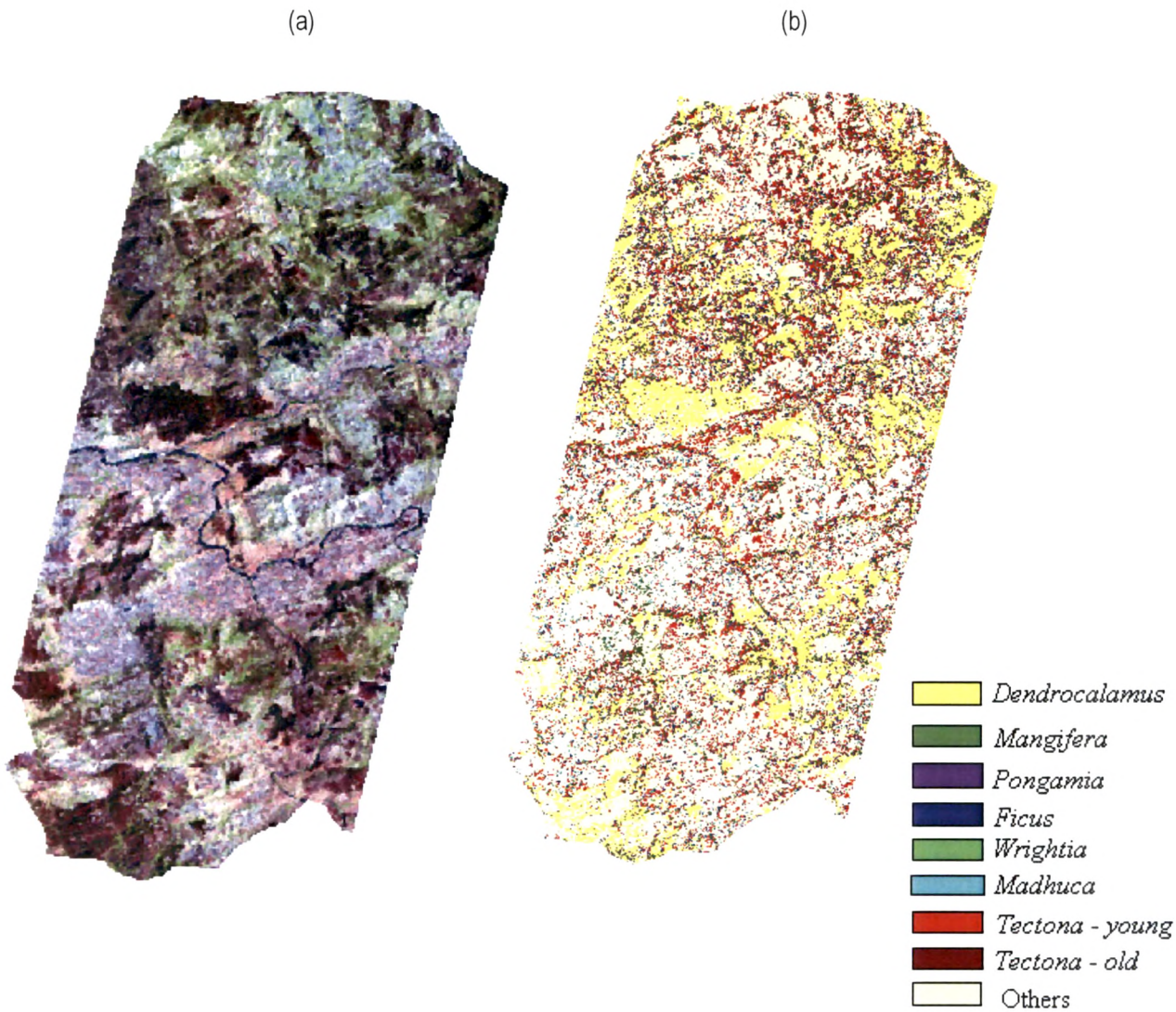

Figure 12: Shoolpaneshwar wildlife sanctuary (a) Area of interest using selected three sensitive bands (RGB): 1628nm, 962nm, 681nm, (b) image of supervised classification using selected (3) sensitive bands

Table 2: Area occupancy (from supervised classification image) along with probability values, and pixel numbers used for accuracy assessment

Class	Probability of occupancy ($\sum p=1$)	Area in hectare	Area in %	Correctly Classified pixels	Validated pixels used
Dendrocalamus strictus	0.07	1753	13.6	4	6
Mangifera indica	0.06	725	5.63	3	5
Pongamia pinnata	0.05	601	4.66	3	4
Ficus glomerata	0.03	378	2.93	2	4
Wrightia tinctoria	0.04	321	2.49	2	5
Madhuca indica	0.05	312	2.42	3	6
Tectona grandis (Young)	0.13	889	6.90	4	5
Tectona grandis (Old)	0.13	835	6.48	4	6
Others	0.44	7062	54.84	9	15
Total	1	12876	99.95	34	56

Table 3: Accuracy assessment report.* Boldface values indicate the number of correctly classified samples

Class	Field Survey Data									Total	User's accuracy
	Dendro calamus	*Mangifera*	*Pongamia*	*Ficus*	*Wrightia*	*Madhuca*	*Tectona* (old)	*Tectona* (young)	others		
Dendrocalamus	**4**	2	-	-	-	-	-	-		6	66.6
Mangifera	1	**3**	1	-	-	-	-	-	-	5	60.0
Pongamia	-	-	**3**	-	-		1		-	4	75.0
Ficus	-	-	1	**2**	-	-	1	-	-	4	50.0
Wrightia	-	-	-	-	**2**	-	2		1	5	40.0
Madhuca	-	-	-	-		**3**	-	-	3	6	50.0
Tectona (old)	-	-	-	-	-	1	**4**		1	6	66.6
Tectona (young)	-	-	-	-	-	-		**4**	1	5	80.0
others	-	-	-	-	1	2	3	-	**9**	15	60.0
Total	5	5	5	2	3	6	11	4	15	**56**	-
Producer's accuracy	80.0	60.0	60.0	100.0	66.6	50.0	36.3	100.0	60.0		

(a)

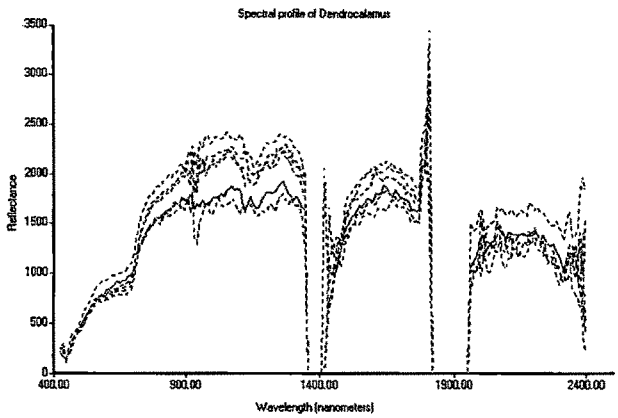
Spectral profile of Dendrocalamus
Reflectance
3500
3000
2500
2000
1500
1000
500
0
400.00
900.00
1400.00
1900.00
2400.00
Wavelength (nanometers)

(b)

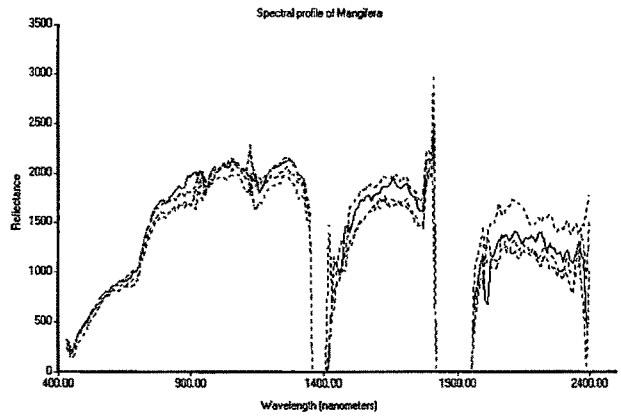
Spectral profile of Mangifera
Reflectance
3500
3000
2500
2000
1500
1000
500
0
400.00
900.00
1400.00
1900.00
2400.00
Wavelength (nanometers)

(c)

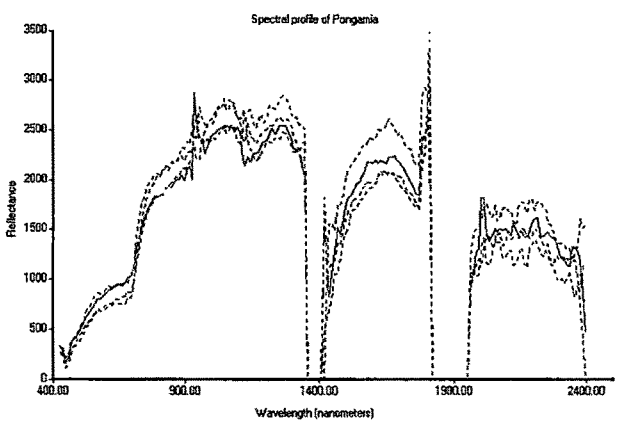
Spectral profile of Pongamia
Reflectance
3500
3000
2500
2000
1500
1000
500
0
400.00
900.00
1400.00
1900.00
2400.00
Wavelength (nanometers)

(d)

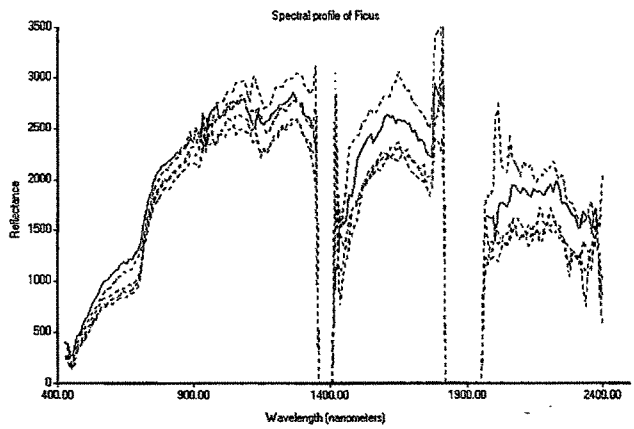
Spectral profile of Ficus
Reflectance
3500
3000
2500
2000
1500
1000
500
0
400.00
900.00
1400.00
1900.00
2400.00
Wavelength (nanometers)

(e)

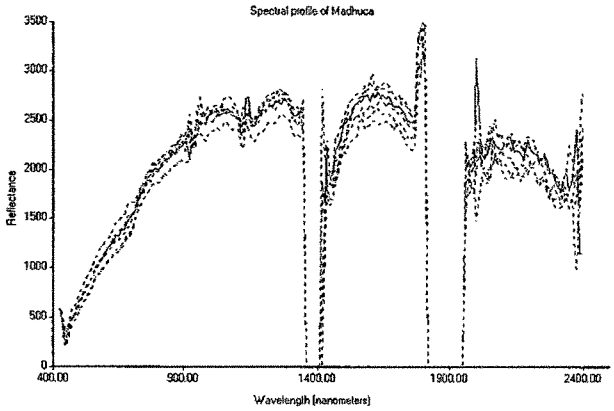

(f)

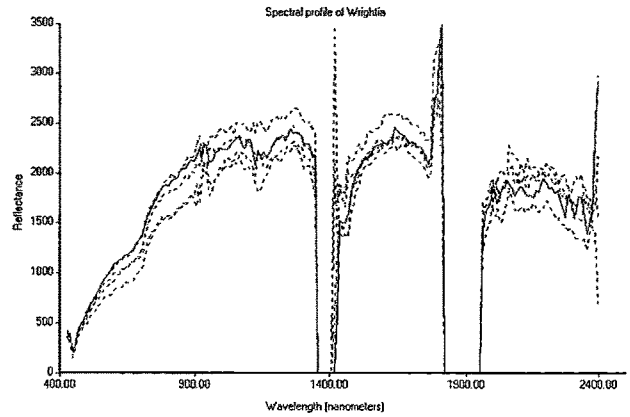

(g)

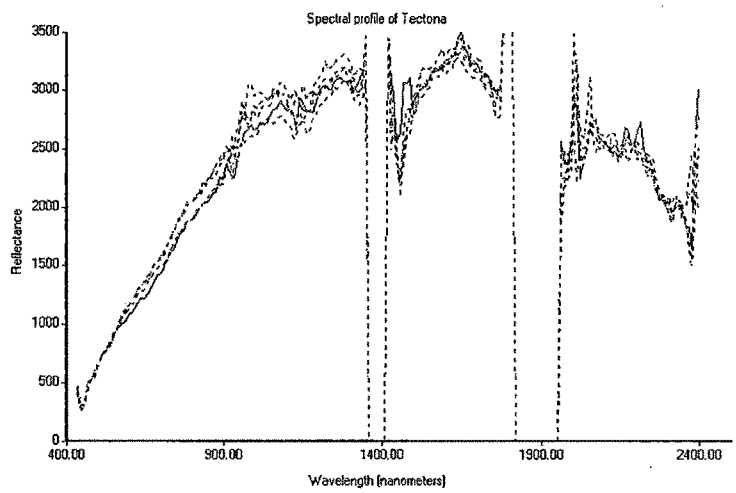

Figure 13: Descriptive spectra (——) along with other spectra (-----) coming from the same for each species seen in the cluster.

3.7. Species level discrimination using Spectral Angle Mapper (SAM)

This section examines the use of Hyperion data (October month imagery) to classify tropical trees based on entire spectrum, spectrum partition analysis and spectra from MNF (Minimum Noise Fraction) bands using SAM (Spectral Angle Mapper) algorithm. Results are mentioned in Tables (4-11) & Figures (14-19). Results indicate about the intricacies and limitations involved in extraction of information for tropical vegetation from Hyperion sensor.

3.7.1. MNF transformation

Original Hyperion bands were compared to the MNF (Minimum Noise Fraction) transformed bands. From figure 14 strong correlations were apparent between the first six bands of original Hyperion data. Whereas the first five MNF bands showed strong spatially coherent contrasts illustrating spectral distinction between water, shadows, elevation, vegetation etc. and the high order MNF bands showed consistently diminishing spatial coherence (MNF Band-6 onwards). The eigenvalue plot shown in figure 15 verifies that the first five MNF bands contain most of the spatially coherent variance. Eigenvalues were ranging from 11.20 to 1.44. The MNF analysis on the Hyperion image showed that the first eigenimage had an eigenvalue of 11.2, by the 9th eigenimage the eigenvalue dropped to 3.13 and after the 33 eigenvalues became asymptotic at 1.9. Further by the 19th eigenimage most of the structural features of the forest disappeared, indicating high noise content. Plot showed the eigenvalue for each MNF transformed band (Figure 15). Here larger eigenvalues indicate higher data variance in the transformed band and as eigenvalue approached 1 only noise was left in the transformed band.

3.7.2. Pixel Purity Index (PPI)

Using high variance MNF band combinations PPI was developed (Figure 16). Table 4 gives an idea about the data value (the number of times that pixel was recorded as an extreme) range and number of pure pixels in each selected MNF band combinations. Highest data value range with lowest number of pure pixels recorded when PPI was developed using 1st and 2nd MNF bands. While lowest data value range with highest number of pure pixels recorded when PPI was developed using 1-15 MNF bands. In figure 16, PPI images from high variance MNF bands showed distinct pattern of pure pixels owing to their spatial coherence. As mentioned in the chapter

2 section 5.2.2, the field observations were overlaid on each selected band combinations given in table 5 for each species. Number of purest pixels and hits for each species were observed and data value/number of iterations for each of these pixels was recorded. Band combination was different for different species. Field observations for species like *Tectona* and *Dendrocalamus* showed higher number of hits in 1-5 MNF band combination as they are homogeneously distributed. While for others it was in 1-10 MNF band combination. Hence, 1-5 MNF band combination was used as an unique band combination to select correct endmember for *Tectona* and *Dendrocalamus* for subsequent analysis. For other species, 1-10 band combination was used to select endmember spectra. Here data processing showed the advantages of MNF transform followed by the development of PPI. These transformations helped in minimizing data dimensionality. It also helped in the extraction of endmember spectra from field-based measurements for each species.

3.7.3. Endmember spectra

Five endmembers were defined in the PPI driven approach. Pixel locations having maximum number of iterations were considered as endmember for respective species such as *Tectona* (PPI= 745), *Dendrocalamus* (PPI= 203), *Mangifera* (PPI= 38), *Madhuca* (PPI= 24) and *Ficus* (PPI= 49). Figure 17 showed reflectance spectra of 5 selected tropical tree species. Endmembers of 5 selected tree species had a distinct red edge, chlorophyll absorption in VIS wavelengths, higher reflectance in NIR and decreased reflectance in the SWIR wavelengths due to water absorption (Figure 17a). Figure 17b showed 5 selected endmember spectra extracted using MNF bands. These spectra were used as library spectra for the classification of selected tropical tree species.

3.7.4. SAM (Spectral Angle Mapper) classification

The Hyperion image was classified using SAM algorithm with the help of above selected PPI driven endmember spectra as different classes of five tropical tree species. SAM was performed for the entire spectrum, spectra from VIS-NIR region (1-90bands), SWIR-I region (103-136bands), SWIR-II region (159-195bands), 1-10 MNF and 1-15 MNF bands. In this study, SAM classification was accomplished by assigning each sample spectrum to the class with the closest similarity (i.e. lowest spectral angle) and no maximum angle threshold was used to minimize false detection. The

resulting classified images are shown in figure 18. SAM proved to be a good algorithm for classifying tropical trees. Further, the accuracy of the classified images were evaluated by generating a contingency matrix using 141 independent reference samples, which were not part of the reference samples used for the development of the endmember/library spectra (Tables 6-11). SAM classification with 196bands (full-spectra) of Hyperion data gave 51% OAA with 0.47 KAPPA for the 5 selected tropical trees. User's and producer's accuracies were ranging from 22.22%-82.35% and 35.71%-61.53% respectively (Table-6). Partition analysis across the spectrum was done for three regions (VIS-NIR, SWIR-I, SWIR-II). VIS-NIR region was taken together to give emphasis for red edge variations as the canopy is lush green. VIS-NIR bands performed well with an OAA of 54.60% and 0.45 KAPPA. OAA was maximum at VIS-NIR indicating its superiority in classification. User's and producer's accuracies were ranging from 31.25%-74.50% and 27.77%-72.7% respectively (Table-7). OAA for other two regions (SWIR-I & II) were 33.33% and 26.24% respectively. OAA was minimal for spectra of SWIR-II region. Results are given in tables 6-9.

Images coming from spectra of MNF bands were much sharper compared to others (Figures 19b & 19c). SAM gave 55.31% OAA with 0.46 KAPPA using 1-15 MNF bands. User's and producer's accuracies were ranging from 38.84%-70.58% and 70%-85.71% respectively (Table-10). Finally SAM showed the highest overall accuracy of 59.57% with 0.51 KAPPA using spectra of 1-10MNF bands. This higher OAA indicated the potential of hyperspectral imagery for tropical tree species discrimination using SAM. User's and producer's accuracies were ranging from 42.10%-72.54% and 66.66%-82.22% respectively (Table-11) indicating a wider difference in the classification accuracy of the selected tropical tree species. From table11 & 12 it was observed that by using spectra from 1-10 and 1-15 MNF bands misclassification could be minimized which led to increase in producer's and user's accuracies for each class. Consequently highest producer's accuracy was observed using spectra of 1-15MNF bands compared to other 5 band combinations. Likewise highest User's accuracy was achieved using spectra of 1-10 MNF bands.

Accuracy levels at all spectral scale were highest for *Tectona* which was followed by *Dendrocalamus* owing to their homogenous distribution in larger areas (Tables-7, 8, 11 & 12). Surprisingly, SAM had achieved relatively good performance using entire spectrum for *Tectona* (Table-6). While, accuracy levels at all scales were lowest for *Madhuca, Mangifera* (distributed

close to cultivated areas) and *Ficus* (distributed near water body and road side). Further it was evident that accuracy levels for all 5 species were lower using spectra from SWIR-I & II bands (Table 8 & 9).

Results clearly indicate that SAM can achieve relatively good performance for homogenous species at all spectral scale. Present results confirm the benefits of homogenous patches over heterogeneous patches

Hyperion Band-1

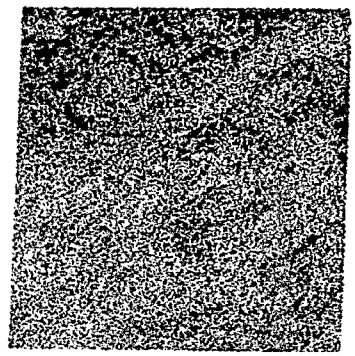

MNF Band-1

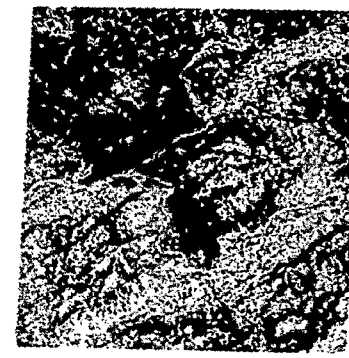

Hyperion Band-2

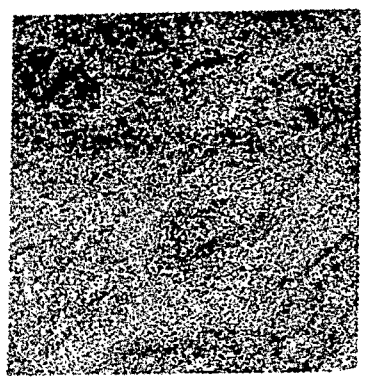

MNF Band-2

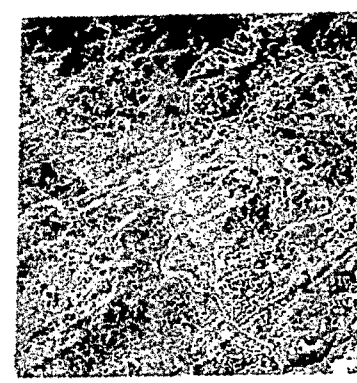

Hyperion Band-3

MNF Band-3

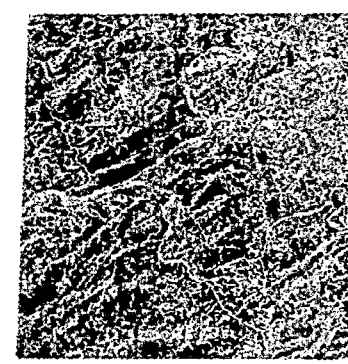

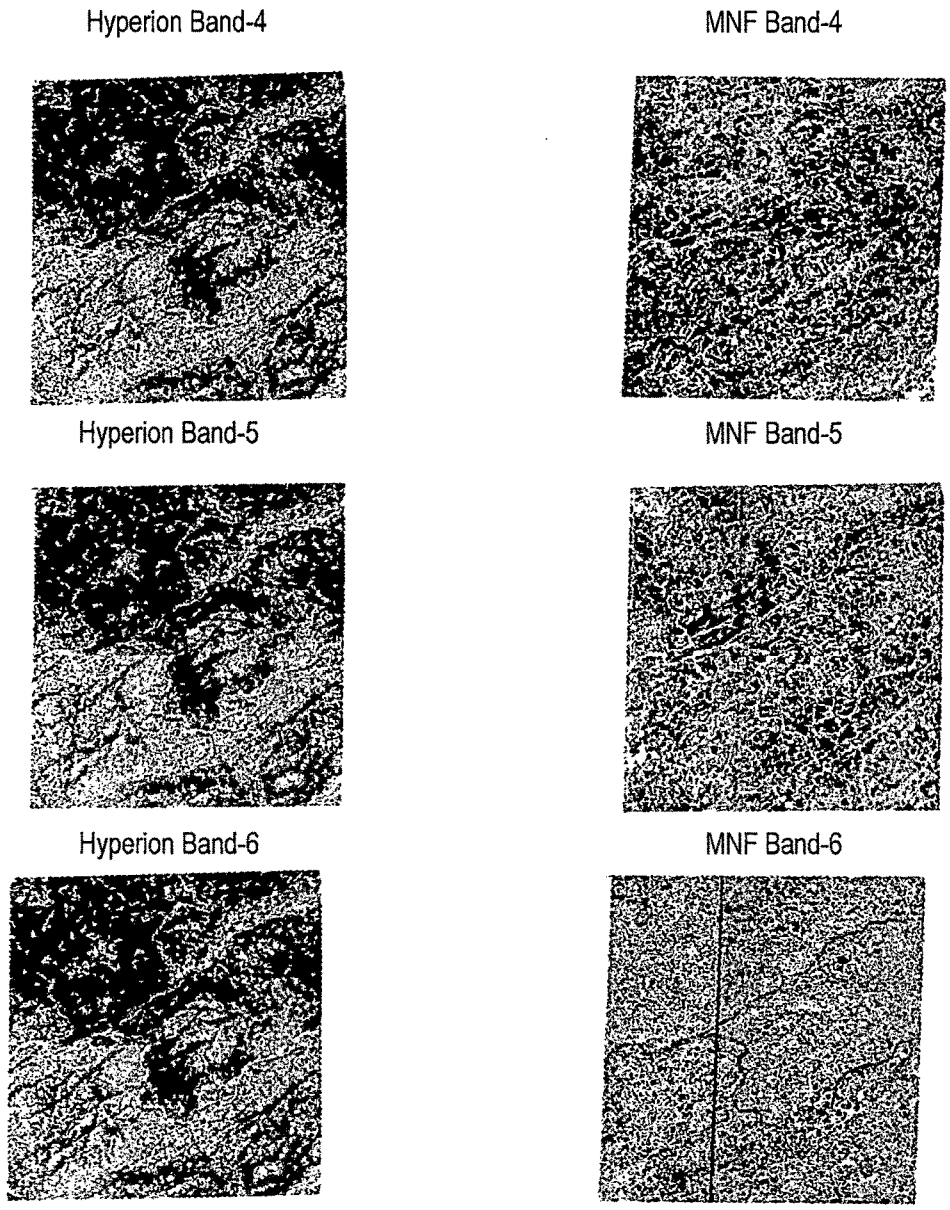

Figure 14: Dimensionality of hyperspectral reflectance of October month imagery. Strong correlation is observed amongst the first six reflective bands of Hyperion data. After applying a Minimum Noise Fraction (MNF) transformation, the spatially coherent variance is contained in the low-order components (MNF Bands 1-5) while the spatially uncorrelated variance relegates the higher order components (MNF Band 6 onwards). Total information content is invariant under the transformation.

(a) (b)

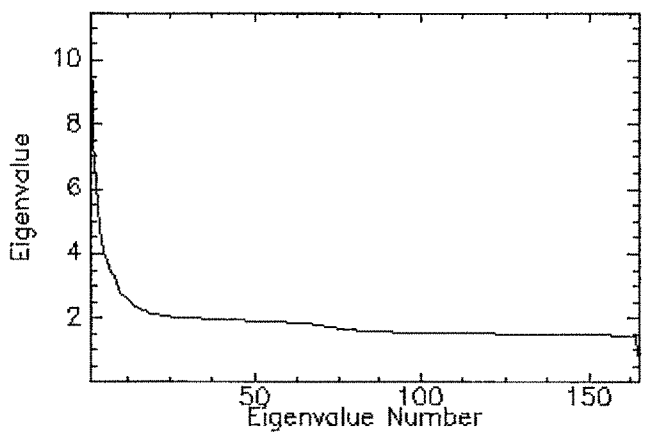

Column 1: Eigenvalue Number	Column 2: Eigenvalues---1
1.000000	11.207144
2.000000	7.501681
3.000000	6.209252
4.000000	4.742379
5.000000	4.035851
6.000000	3.791635
7.000000	3.559026
8.000000	3.369550
9.000000	3.132602
10.000000	2.801804
11.000000	2.739019
12.000000	2.634007
13.000000	2.540571
14.000000	2.454446
15.000000	2.387923
16.000000	2.332352
17.000000	2.266138
18.000000	2.249562
19.000000	2.162192
20.000000	2.133433
21.000000	2.123918
22.000000	2.105908
23.000000	2.088357
24.000000	2.057143
25.000000	2.054517
26.000000	2.043249
27.000000	2.028509
28.000000	2.016467
29.000000	2.013798
30.000000	2.012121
31.000000	2.006763
32.000000	2.002875
33.000000	1.992483
34.000000	1.990334
35.000000	1.985946

Figure 15: a) The eigenvalue spectrum corresponding to MNF transformed bands shown in figure 19 indicates that the first 5 components contain the majority of the spatially correlated variance compared to the other low order components,

b) Eigenvalue in text format

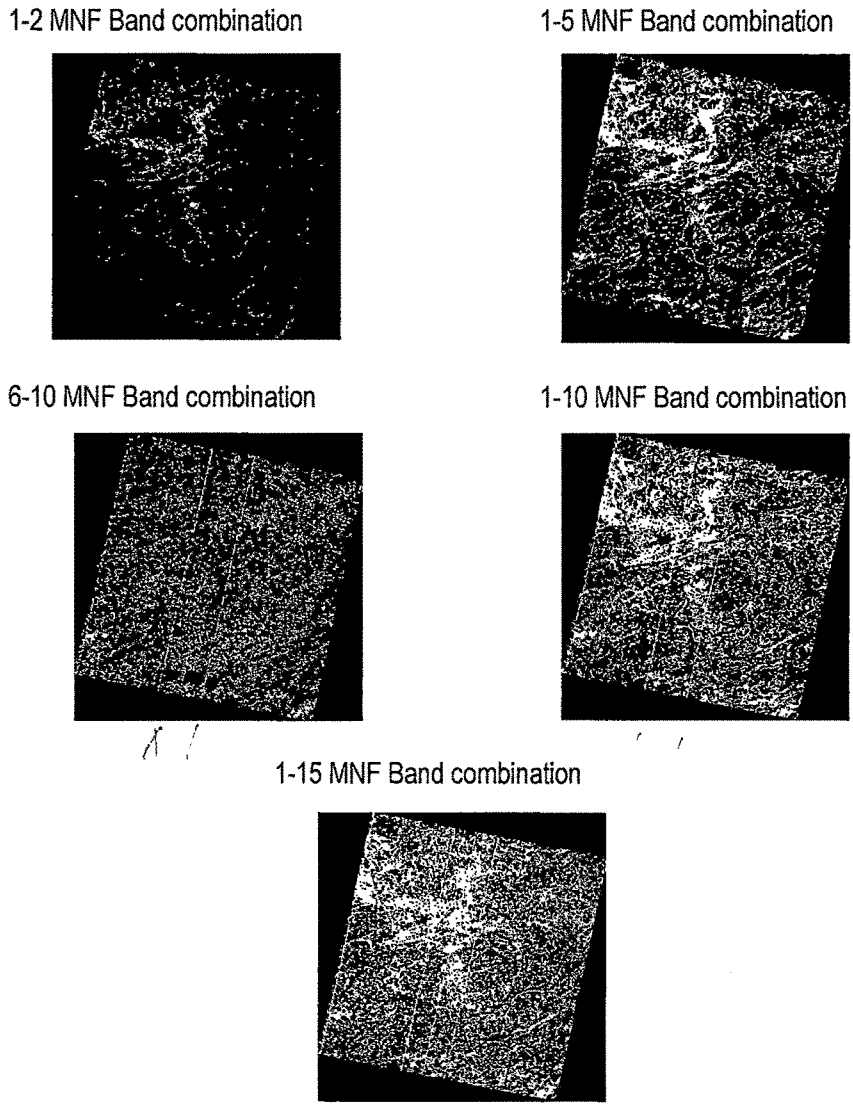

Figure 16: Developed PPI (Pixel Purity Index) images from selected different MNF band combinations.

(a)

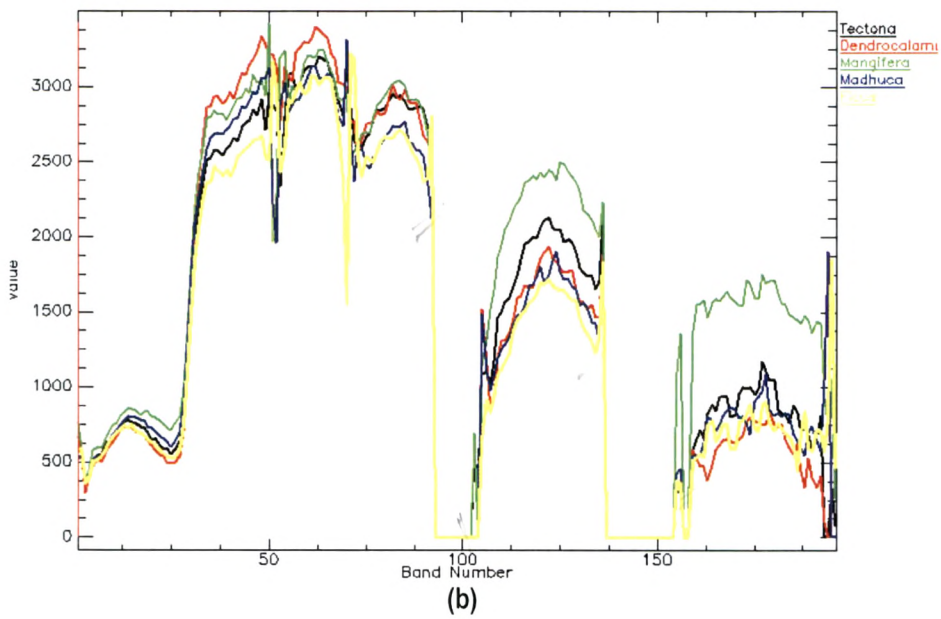

(b)

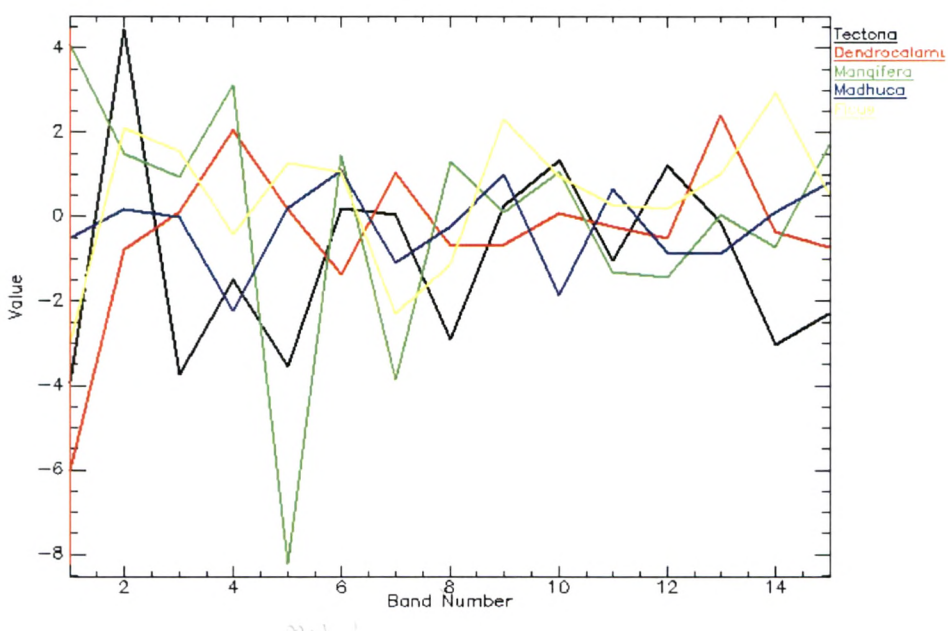

Figure 17: Endmember spectra of 5 selected tree species extracted using (a) all 196 bands and (b) MNF bands

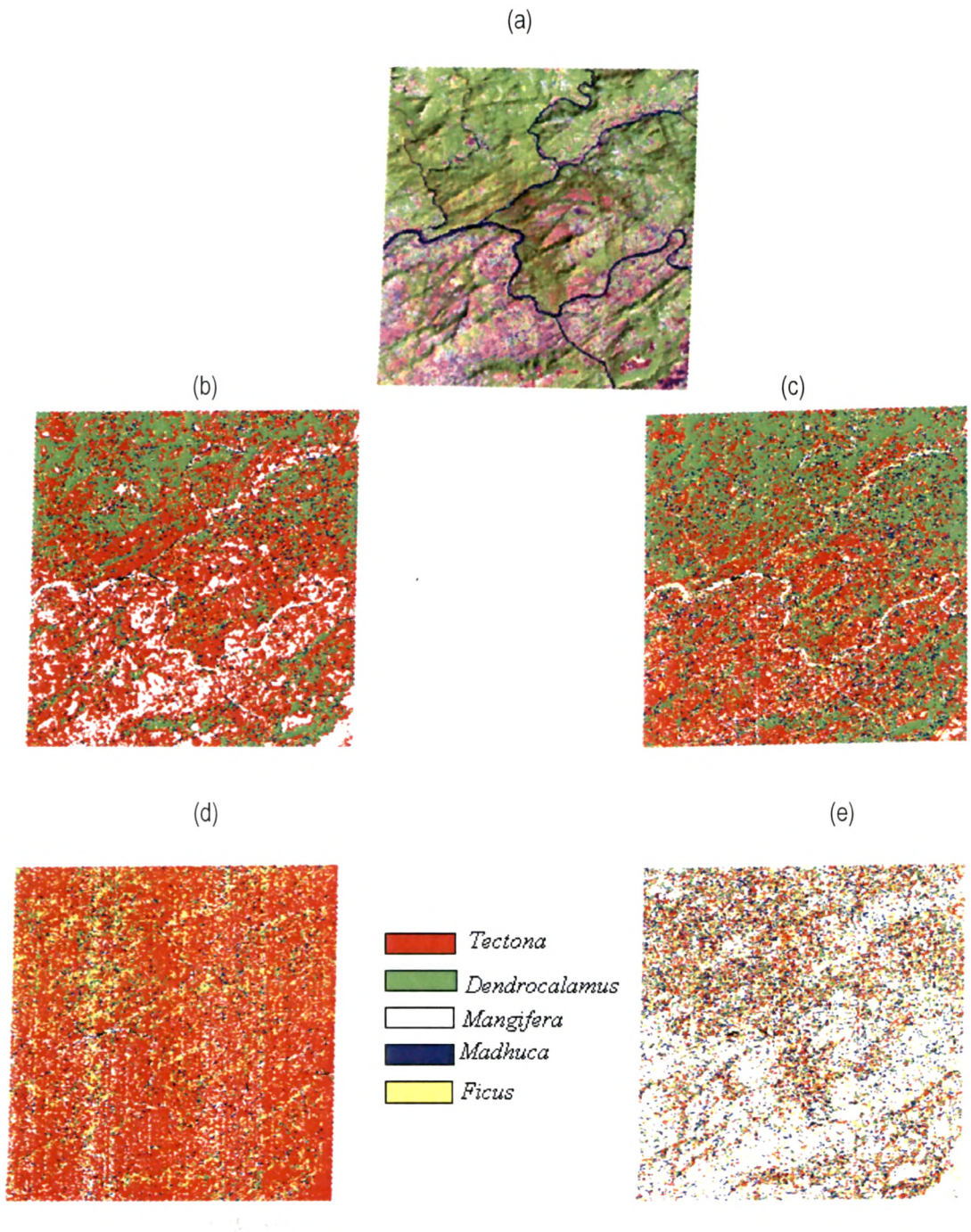

Figure 18: Input data (a) Hyperion data (Color composite: SWIR-II-1648NM; NIR- 833nm; RED-660nm), results of SAM algorithm using (b) full spectrum (1-196bands) (c)VIS-NIR region (1-90bands), (d) SWIR-1 region (103-136bands), (e) SWIR-II region (159-195bands).

(a)

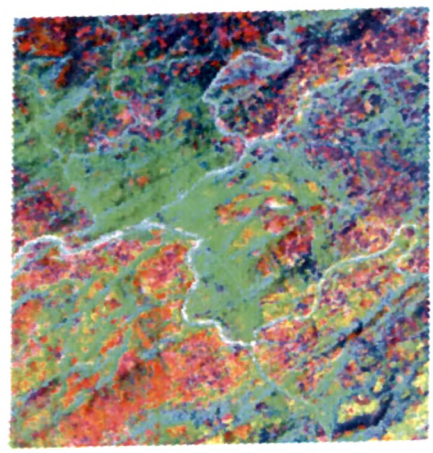

(b)

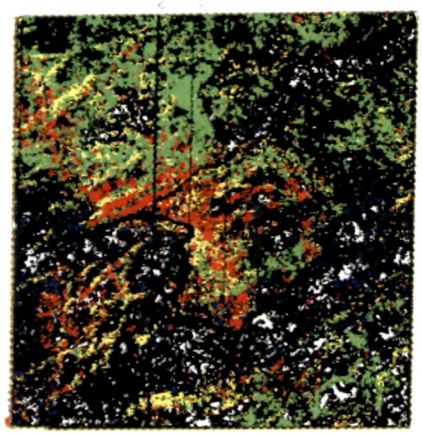

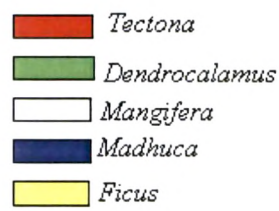

(c)

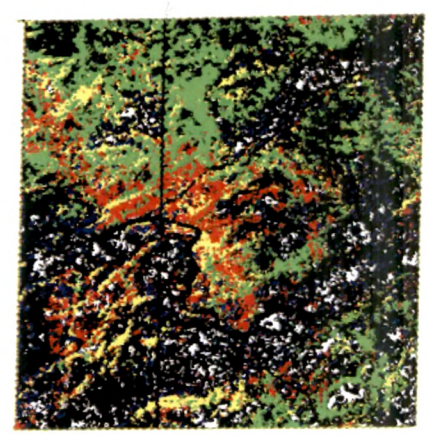

Figure 19: Input data (a) MNF transformed data (Color composite of MNF bands 1, 2 & 3), results of SAM algorithm using (b) 1-15 MNF bands & (c) 1-10 MNF bands.

Table 4: Datavalue range and number of pure pixels coming from selected MNF band combinations

MNF Band combinations	Range of data value	Pure pixels
1-2	1-6199	3541
1-3	1-5551	8552
1-4	1-5201	17696
1-5	1-4521	20707
1-6	1-3684	28599
1-7	1-3495	30216
1-8	1-3118	32231
6-10	1-3821	14134
1-10	1-2892	30019
1-15	1-2997	35677

Table 5: OAA & KAPPA using different band combination at different angle

Band combinations	Angle	OAA	KAPPA
196bands	None	51.06	0.477
VIS-NIR (1-90bands)	None	54.60	0.450
SWIR-I	None	33.33	0.251
SWIR-II	None	26.24	0.222
1-15MNF bands	None	55.31	0.467
1-10MNF bands	None	59.57	0.519

Table 6: Accuracy assessment report generated from SAM algorithm using 196 bands.* Boldface values indicate the number of correctly classified samples.

Class	Field Survey Data						Total	User's accuracy
	Tectona	*Dendro calamus*	*Mangifera*	*Madhuca*	*Ficus*	Unclassified		
Tectona	**42**	2	1	3	3		51	82.35
Dendrocalamus	15	**15**	1	1	5	-	37	40.54
Mangifera	5	5	**8**	1	-	-	19	42.10
Madhuca	11	2	-	**4**	1	-	18	22.22
Ficus	5	2	3	1	**5**	-	16	31.25
Total	78	26	13	10	14	-	**141**	
Producer's accuracy	53.84	57.69	61.53	40	35.71	-		

Table 7: Accuracy assessment report generated from SAM algorithm using VIS-NIR bands.* Boldface values indicate the number of correctly classified samples.

Class	Field Survey Data						Total	User's accuracy
	Tectona	*Dendro calamus*	*Mangifera*	*Madhuca*	*Ficus*	Unclassified		
Tectona	**38**	3	4	1	5		51	74.50
Dendrocalamus	11	**18**	1	2	5	-	37	48.64
Mangifera	5	6	**6**	-	2	-	19	31.57
Madhuca	3	2	4	**8**	1	-	18	44.44
Ficus	6	2	3	-	**5**	-	16	31.25
Total	63	31	18	11	18	-	**141**	
Producer's accuracy	60.31	58.06	33.33	72.7	35.71	-		

Table 8: Accuracy assessment report generated from SAM algorithm using SWIR I bands.*

Boldface values indicate the number of correctly classified samples.

Class	Field Survey Data						Total	User's accuracy
	Tectona	*Dendro calamus*	*Mangifera*	*Madhuca*	*Ficus*	Unclassified		
Tectona	**36**	5	2	5	3		51	70.58
Dendrocalamus	13	**7**	4	4	9	-	37	18.91
Mangifera	12	2	**2**	1	2	-	19	10.52
Madhuca	12	2	2	**1**	1	-	18	5.55
Ficus	10	1	3	-	**2**	-	16	12.5
Total	83	17	13	11	18	-	**141**	
Producer's accuracy	43.37	41.17	15.38	9.09	11.11	-		

Table 9: Accuracy assessment report generated from SAM algorithm using SWIR-II bands.*

Boldface values indicate the number of correctly classified samples.

Class	Field Survey Data						Total	User's accuracy
	Tectona	*Dendro calamus*	*Mangifera*	*Madhuca*	*Ficus*	Unclassified		
Tectona	**7**	3	26	7	7		51	13.72
Dendrocalamus	5	**6**	14	4	9	-	37	19.35
Mangifera	2	-	**15**	1	1	-	19	78.94
Madhuca	3	-	10	**3**	2	-	18	16.66
Ficus	-	-	8	1	**7**	-	16	43.75
Total	17	9	73	16	25	-	**141**	
Producer's accuracy	41.17	66.66	20.54	18.75	28	-		

Table 10: Accuracy assessment report generated from SAM algorithm using 1-15 MNF bands.* Boldface values indicate the number of correctly classified samples.

Class	Field Survey Data						Total	User's accuracy
	Tectona	*Dendro calamus*	*Mangifera*	*Madhuca*	*Ficus*	Unclassified		
Tectona	**36**	4	-	3	-	8	51	70.58
Dendrocalamus	5	**19**	1	-	3	9	37	51.35
Mangifera	1	-	**7**	-	-	11	19	36.84
Madhuca	-	-	-	**8**	-	10	18	44.4
Ficus	-	-	1	-	**7**	8	16	43.75
Total	42	23	9	11	10	46	**141**	
Producer's accuracy	85.71	82.60	77.77	72.72	70			

Table11: Accuracy assessment report generated from SAM algorithm using 1-10 MNF bands.* Boldface values indicate the number of correctly classified samples.

Class	Field Survey Data						Total	User's accuracy
	Tectona	*Dendro calamus*	*Mangifera*	*Madhuca*	*Ficus*	Unclassified		
Tectona	**37**	5	1	1	2	5	51	72.54
Dendrocalamus	7	**22**	1	-	2	5	37	59.45
Mangifera	1	-	**8**	-	-	10	19	42.10
Madhuca	-	-	-	**8**	-	10	18	44.44
Ficus	-	1	2	-	**9**	4	16	56.25
Total	45	28	12	9	13	34	**141**	
Producer's accuracy	82.22	78.57	66.66	88.8	69.23			

3.8. Forest floor studies

Forest floor study was performed using dry season Hyperion imagery to discriminate bare soil from litter layer. To distinguish litter cover of different thicknesses, spectra were extracted from points with different loads of litter. This helped in looking at the load factor of litter for a potential forest fire. Variations in spectral characteristics of different types of leaf litter were seen. Spectral reflectance curves were different for different thicknesses of leaf litter. Thus, spectra differed as the thickness varied. Spectral profile for *Tectona, Dendrocalamus* and mixed cover showed that as thickness increased reflectance also increased (Figure 20a; Figure 21a; Figure 22a). Altitude of the terrain had an influence on the reflectance of litter. As altitude increased reflectance also increased for *Tectona* and mixed deciduous species (Figure 20b; Figure 22b) where as in *Dendrocalamus* as altitude increased reflectance decreased (Figure 21b). Altitude variation in the reflectance curves of bare soil was also seen.

In figure 23a, descriptive spectra of *Dendrocalamus* and other mixed deciduous species were discernable from same leaf litter thickness (5-7cm) whereas *Dendrocalamus* (5-7cm) and *Tectona* (8-10cm) showed lesser separation in visible wavelengths while more separation in NIR and SWIR wavelengths. Similar observations were seen in figure 24a, where *Tectona* (9-11cm) showed more separation with other mixed deciduous species (9-11cm) and lesser separation with Den*drocalamus* (7-9cm), except for VIS wavelengths. To distinguish different types of litter cover, spectra were extracted from points with same thickness (10-15cm) at same altitude (Figure 25). Soil spectra also were plotted to observe separation. Soil reflectance was significantly different at all wavelengths except in the VIS region. Common spectral features in both plant litter and soils are two broader water absorption bands at 1400nm and 1900nm. Each spectrum is unique for that cover type. From descriptive spectra (Figure 23 & Figure 24) it was observed that all four categories showed similar pattern in NIR and SWIR region with slight variation in VIS region. This at times was not sufficient to discriminate different types of forest cover from soil.

3.8.1. Continuum removal

In order to differentiate them better the same had been plotted as continuum removal spectra. Continuum removal spectra were also extracted for these four types. In this study the continuum

removed spectra (Figure 23b; Figure 24b; Figure 25b) clearly showed several distinguishable absorption features for *Tectona, Dendrocalamus* and mixed dry species while the spectra of bare soil showed no absorption. The predominant absorption features were found in visible (500-690nm) and the SWIR-II (2050-2400nm) wavelengths (Figures 23b, 24b, 25b) where discrimination can be easily done. In figure 25b it can be seen that *Tectona* and bare soil spectra can be discernable in the visible region while *Dendrocalamus* and other mixed dry species show similar absorption feature. Further in figure 25b all 4 types were distinctly separable. Separation was very clear at VIS and SWIR-II wavelengths. Further all 4 can be easily discernable in the SWIR II wavelengths. Here SWIR-II wavelengths are more sensitive to the type of floor cover indicating its distinctiveness. Sharp absorption features were seen in VIS and SWIR-II wavelengths which were absent in the spectra of bare soil, indicating the ability of Hyperion data to discriminate dry forest floor from bare soil. Finally, results indicate that four categories such as *Dendrocalamus, Tectona,* mixed dry species and soil can be easily separable from VIS and SWIR II regions (Figure 25b).

3.8.2. Cover type classification

To discriminate these 4 cover types maximum likelihood classification was performed. Bands were selected using continuum removal spectra (Figure 25b). From the continuum removed descriptive spectra, two regions with maximum separation were identified. Selected bands (690nm, 2113nm & 2234nm) are coming from VIS & SWIR-II regions (Figure 26a). At band 701nm all 4 cover types showed different absorption features. All four were easily discernable in the SWIR II region of the spectrum. Supervised classification of the subset using maximum likelihood classification from the 3 selected bands (Figure 26b) showed an overall accuracy of 51.9%, with 27 out of 52 samples. User's and Producer's accuracies were ranging from 25%-58.3% and 40%-87.5% respectively (Table 12). Similar to species level classification, accuracy level was better for floor cover of *Tectona* (58.3%) as it was spread at larger areas as pure patches (Table 12). These results indicate the potential of hyperspectral data to discriminate forest floor cover using dry season data.

Table 12: Accuracy assessment report.* Boldface values indicate the number of correctly classified samples

Class	Field Survey Data					Total	User's accuracy
	Tectona	*Dendro calamus*	Mixed type	Soil	Others		
Tectona	**14**	3	-	2	5	24	58.3
Dendrocalamus	2	**9**	2	-	3	16	56.25
Mixed type	-	4	**2**	1	1	8	25.0
Soil	-	-	-	**2**	2	4	50.0
Others	-	-	-	-	-	-	-
Total	16	16	4	5	11	**52**	-
Producer's accuracy	87.5	56.25	50.0	40.0	-	-	

No of Samples is Less
∴ plot pattern may not be representative

(a)

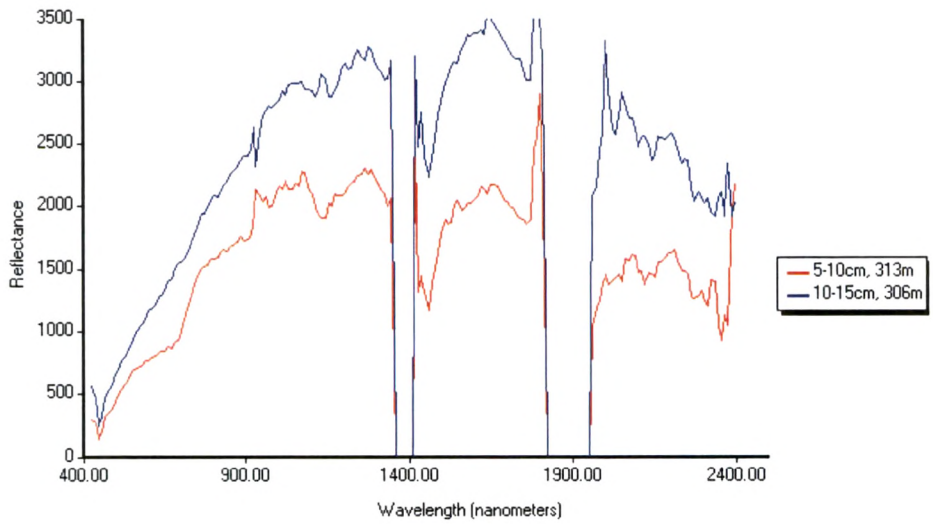

(b)

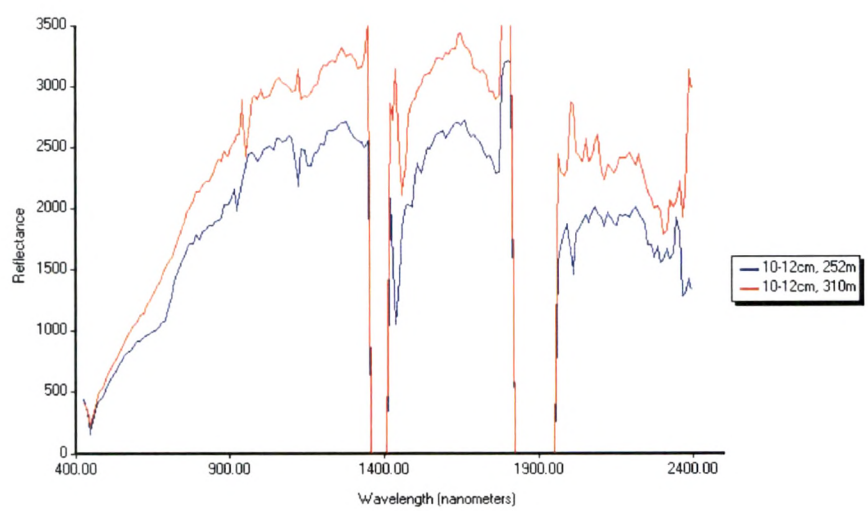

Figure 20: Showing variation in leaf litter thickness of *Tectona grandis* L. (a) spectra from different litter depth at same altitude (b) spectra from same litter depth at different altitude

(a)

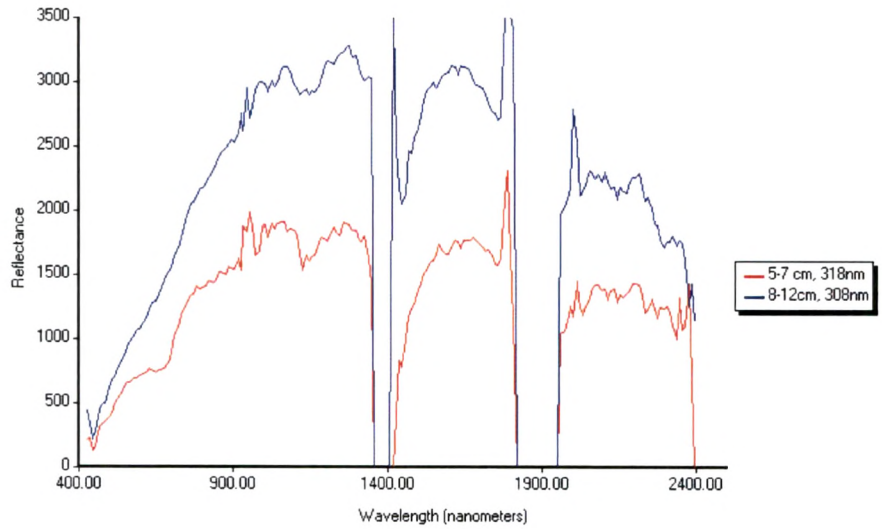

(b)

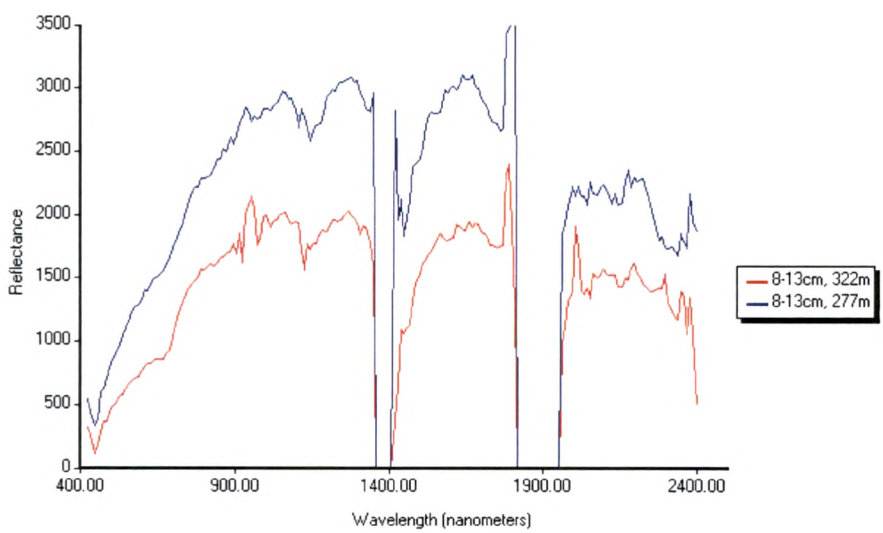

Figure 21: Showing variation in leaf litter thickness of *Dendrocalamus strictus*. (a) spectra from different litter depth at same altitude (b) spectra from same litter depth at different altitude.

(a)

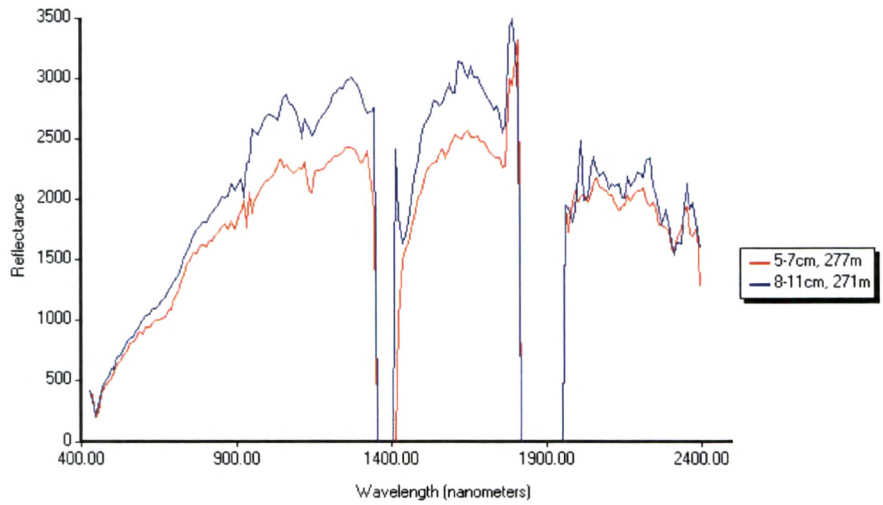

(b)

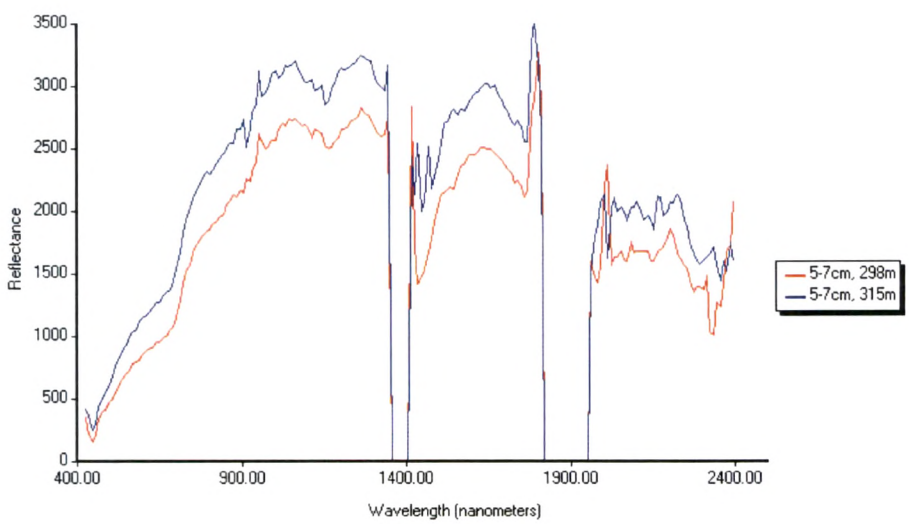

Figure 22: Showing variation in leaf litter spectra of other mixed deciduous species. (a) spectra from different litter depth at same altitude (b) spectra from same litter depth at different altitude.

(a)

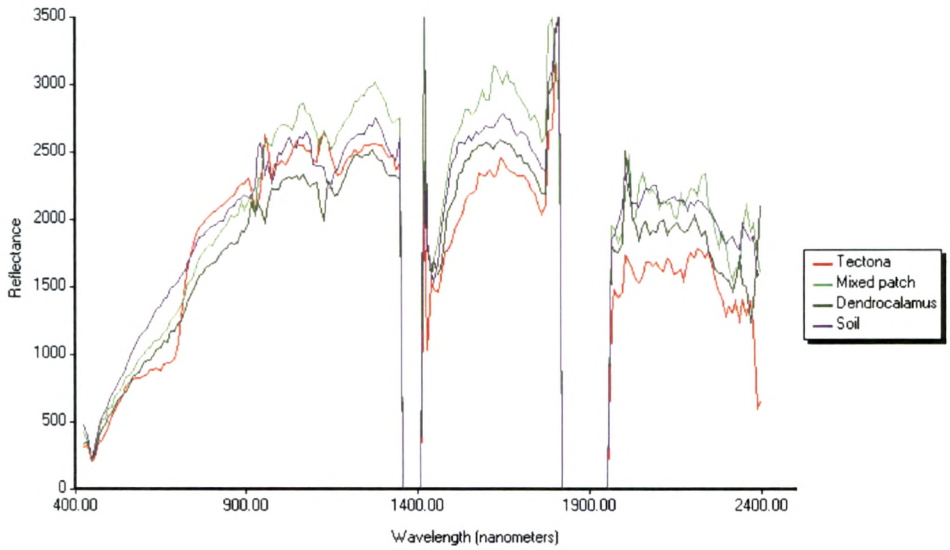

(b)

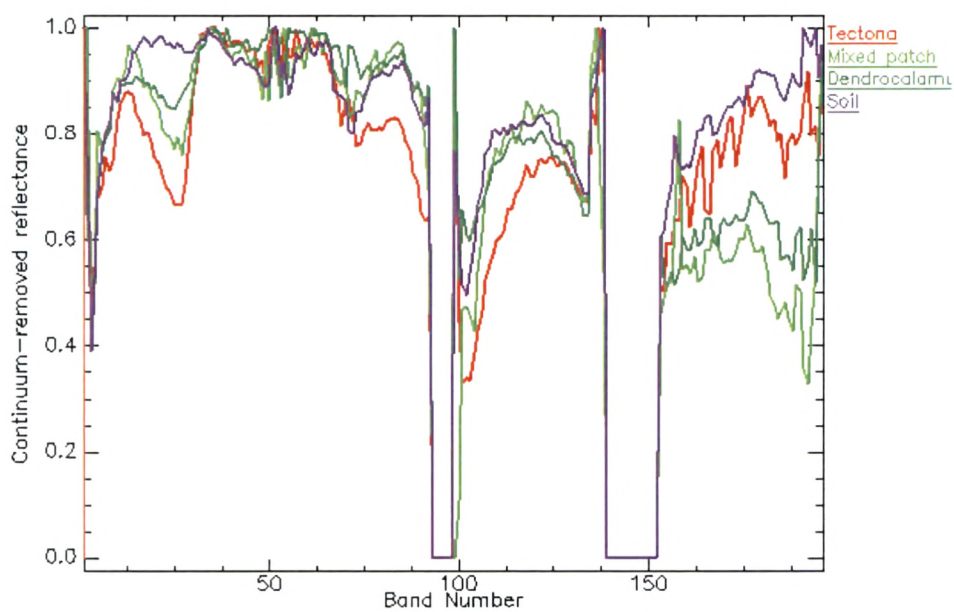

Figure 23: (a) Descriptive spectra, (b) continuum-removed spectra, for Soil, *Dendrocalamus* (5-7cm litter depth); other mixed deciduous species (5-7cm, litter depth) and *Tectona* (8-10cm, litter depth)

(a)

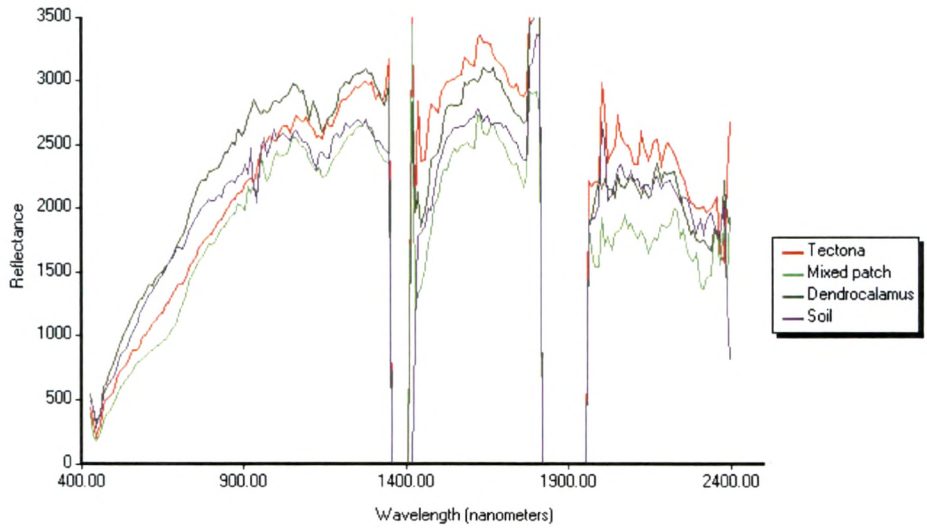

(b)

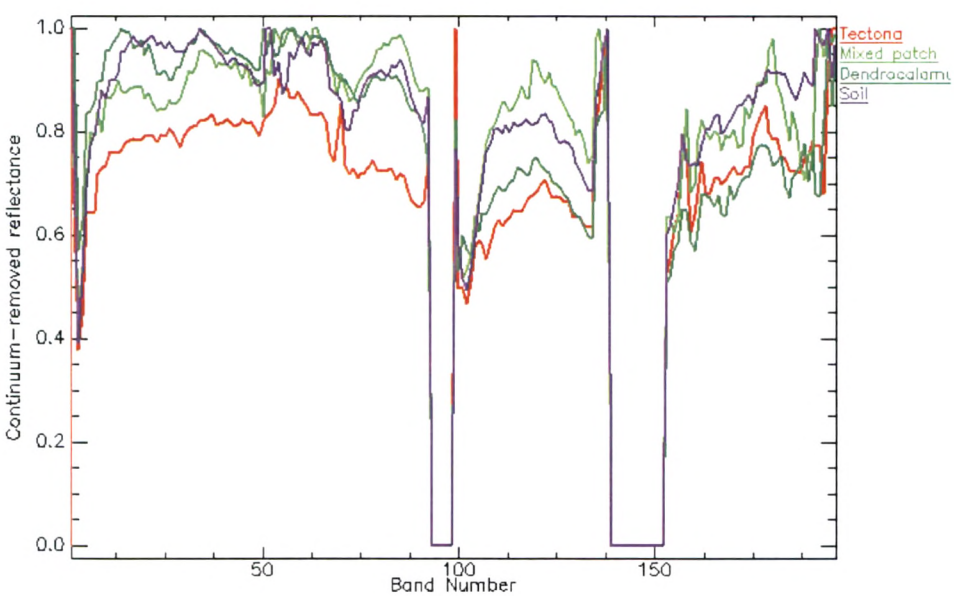

Figure 24: (a) Descriptive spectra, (b) continuum-removed spectra, for Soil, *Tectona* (9-11cm litter depth); other mixed deciduous species (9-11cm, litter depth) and *Dendrocalamus* (7-9cm, litter depth))

(a)

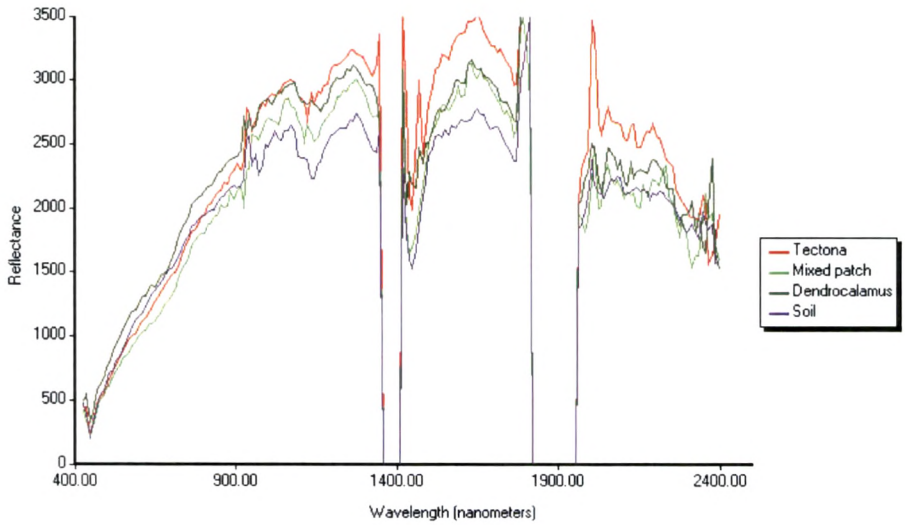

(b)

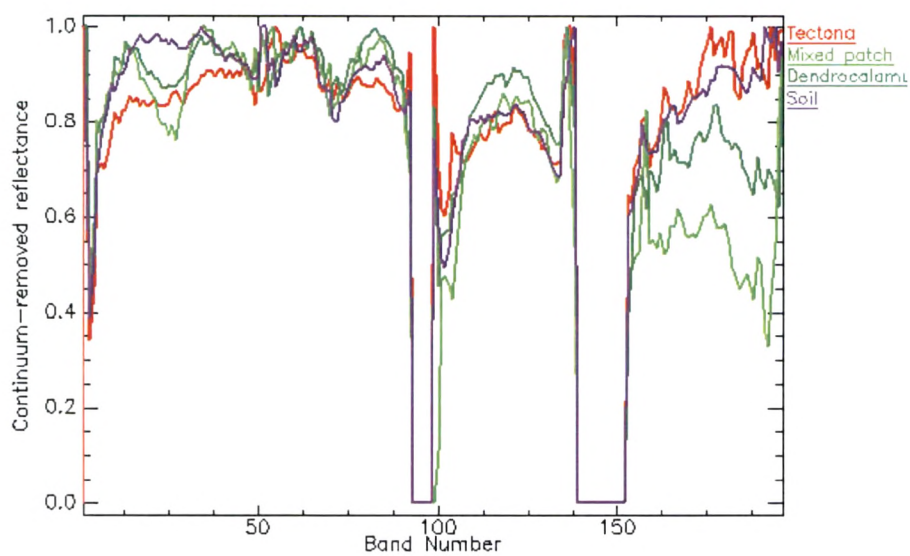

Figure 25: (a) Normal reflectance spectra & (b) Continuum removed spectra for all 4 categories from same litter depth at same altitude.

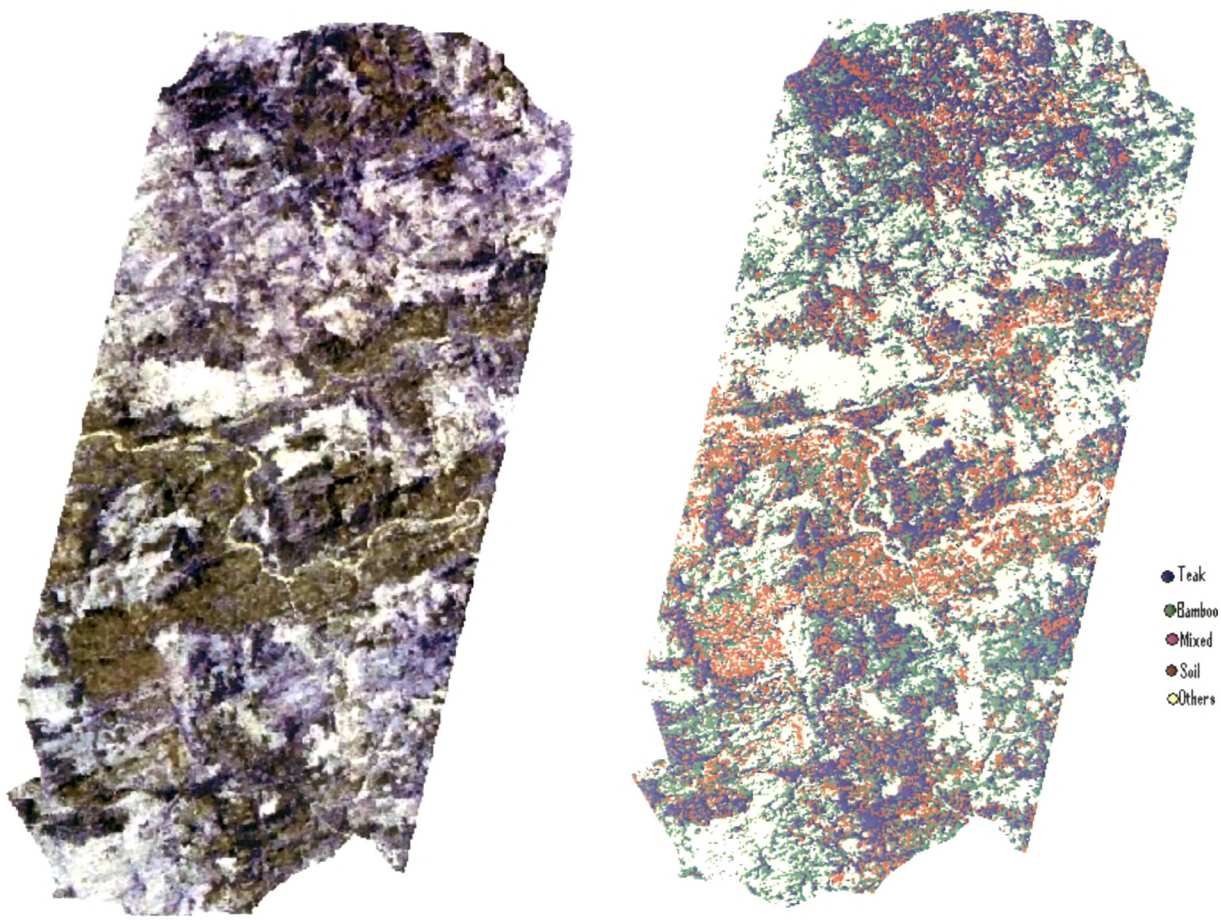

Figure 26: (A) Area of interest using selected three sensitive bands 690nm, 2113nm, 2234nm, (B) image of supervised classification using selected (3) sensitive bands